Final Report Certification
for
CRADA Number ORNL-00-0639

Between

UT-Battelle, LLC

and

Materials Resources, International
(Participant)

Instructions:

Mark the appropriate statement in 1a or 1b below with an 'IX." Refer to the articles in the CRADA terms and conditions governing the identification and marking of Protected CRADA Information.

If no PCI is identified, the report will be distributed without restriction. If PCI is identified, the report distribution will be limited in accordance with the CRADA terms and conditions governing release of data. In all cases items 2 and 3 must be true. That is, the report cannot contain Proprietary Information and a disclosure must be filed prior to release of the report.

This certification may either be made by using this form or may be made on company letterhead if the Participant desires. A faxed copy of this completed form is acceptable.

The following certification is made for the subject final report:

1. (a) The final report contains information that qualifies as "Protected CRADA Information" (PCI). The PCI legend is printed on the report cover, and the PCI is clearly identified.

OR

(b) The final report does not contain "Protected CRADA Information." The "Approved for Public Release" legend is printed on the report cover.

2. The final report does not contain Proprietary Information.

3. By the signature below, the Participant has no objection to the public distribution of the final report due to patentable information.

For the Participant:

Travis M. Wilson
(Name)

App. Engineer/Project Mgr
(Title)

20 May 2004
(Date)

C/ORNL 02-0639

Carbon and Insulation Materials Technology Group
Metals and Ceramics Division

CRADA Final Report
For CRADA Number ORNL 02-0639

Graphite Foam Heat Exchangers for Thermal Management

James Klett
Oak Ridge National Laboratory

Travis Nelson
Materials Resources International
Lansdale, PA

Date Published May, 2004

Prepared by the
OAK RIDGE NATIONAL LABORATORY
Oak Ridge, Tennessee 37831
Managed by
UT-BATTELLE, LLC.
for the
U. S. DEPARTMENT OF ENERGY
under contract DE-AC05-96OR22464

APPROVED FOR PUBLIC RELEASE
UNLIMITED DISTRIBUTION

TABLE OF CONTENTS

LIST OF FIGURES **2**

1. ABSTRACT **3**

2. BENEFIT TO THE DOE'S MISSION **4**

3. PROJECT OBJECTIVES AND WORK PLAN **5**

4. RESULTS **5**

4.1. TASK 1.0 JOINING DEVELOPMENT 5
4.2. TASK 2.0 THERMAL MODELING & TESTING 8
4.3. TASK 3.0 CHIP SCALE PACKAGES 11
4.4. EVAPORATIVE COOLING 15
4.5. TASK 5.0 IGBT PACKAGE COOLING 21

4. INVENTIONS **30**

5. COMMERCIALIZATION POTENTIAL **30**

6. PLANS FOR FUTURE COLLABORATION **30**

7. CONCLUSIONS **30**

8. ACKNOWLEDGEMENTS **30**

9. APPENDIX A: HEAT TRANSFER MODELING **31**

8.1. PROBLEM DEFINITION: 31
8.2. COMPARISON: 34

LIST OF FIGURES

Figure ..... Page

Figure 1. Average Measured Thermal Diffusivity of PocoFoam® and PocoHTC® samples bonded to various substrates. 9
Figure 2. Average Measured Thermal Conductivity of PocoFoam® and PocoHTC® samples bonded to various substrates. 10
Figure 3. Average Measured Thermal Conductivity of PocoFoam® samples bonded to aluminum substrates before and after bonding. 11
Figure 4. Design for 423-pin graphite finned foam heat sink....12
Figure 5. Design for 478-pin graphite finned foam heat sink....12
Figure 6. 423-Cooling Package Thermal Resistance Data....13
Figure 7. 478-Pin Chip Cooler Summary....13
Figure 8. 478-Pin Chip Cooler Bonding Effects....14
Figure 9. 478-Pin Fin Dimension Variation Effects 14
Figure 10. Heat Pipe Design....16
Figure 11. Thermal Resistance of Evaporators vs. Wick Thickness 17
Figure 12. Thermal Resistance of Evaporators vs. Base Heater Power....18
Figure 13. Extended life testing of foam heat pipes. 19
Figure 14. Environmental Compatibility Tests: ΔT vs. Time 20
Figure 15. Heater Power Decrease Effects....21
Figure 16. Design Considerations vs power density. 21
Figure 17. Schematic design of IGBT cooling plate....23
Figure 18. Graphite foam corrugated cold plate with lid. 23
Figure 19. Cold plate test set up. 24
Figure 20 IGBT Coldplate #1 –Water/Glycol 24
Figure 21 IGBT Coldplate #2 –Water/Glycol 25
Figure 22 IGBT Coldplate #3 –Water/Glycol 25
Figure 23 Coldplate #3 – 100% Water....26
Figure 24 Thermal resistance of Water-Cooled, High-Flow, Al/Gr Foam Coldplate 26
Figure 25 Pressure Drop Effects (100% Water in Al/Gr Foam Coldplate)....27
Figure A2. Model geometry for problem descriptor....32
Figure A3. Average heater temperature versus Reynolds number. 35
Figure A4. Thermal resistance of foam compared to Reynolds number for water flow....36
Figure A5. Stanton number versus Reynolds number of the foam with water flow. 37
Figure A6. Thermal resistance versus pumping power....38
Figure A7. Plot of cross section temperature profile. 38
Figure A8. Plot of thermal resistance versus ratio of heat sink height/heat sink length. 39

1. Abstract

Improved thermal management is needed to increase the power density of electronic and more effectively cool electronic enclosures that are envisioned in future aircraft, spacecraft and surface ships. Typically, heat exchanger cores must increase in size to more effectively dissipate increased heat loads, this would be impossible in many cases, thus improved heat exchanger cores will be required. In this Phase I investigation, MRi aimed to demonstrate improved thermal management using graphite foam (Gr-foam) core heat exchangers. The proposed design was to combine Gr-foams from POCO with MRi's innovative low temperature, active metal joining process (S-Bond™) to bond Gr-foam to aluminum, copper and aluminum/SiC composite faceplates. The results were very favorable, so a Phase II SBIR with the MDA was initiated. This had primarily 5 tasks: (1) bonding, (2) thermal modeling, (3) cooling chip scale packages, (4) evaporative cooling techniques and (5) IGBT cold plate development.

The bonding tests showed that the "reflow" technique with S-Bond®-220 resulted in the best and most consistent bond. Then, thermal modeling was used to design different chip scale packages and IGBT cold plates. These designs were used to fabricate many finned graphite foam heat sinks specifically for two standard type IC packages, the 423 and 478 pin chips. These results demonstrated several advantages with the foam. First, the heat sinks with the foam were lighter than the copper/aluminum sinks used as standards. The sinks for the 423 design made from foam were not as good as the standard sinks. However, the sinks made from foam for the 478 pin chips were better than the standard heat sinks used today. However, this improvement was marginal (in the 10-20% better regime). However, another important note was that the epoxy bonding technique resulted in heat sinks with similar results as that with the S-bond®, slightly worse than the S-bond®, but still better than the standard heat sinks.

Next, work with evaporative cooling techniques, such as heat pipes, demonstrated some unique behavior with the foam that is not seen with standard wick materials. This was that as the thickness of the foam increased, the performance got better, where with standard wick materials, as the thickness increases, the performance decreases. This is yet to be completely explained.

Last, the designs from the thermal model were used to fabricate a series of cold plates with the graphite foam and compare them to similar designs using high performance folded fin aluminum sinks (considered standard in the industry). It was shown that by corrugating the foam parallel to fluid flow, the pressure drop can be reduced significantly while maintaining the same heat transfer as that in the folded fin heat sink. In fact, the results show that the graphite foam heat sink can utilized 5% the pumping power as that required with the folded fin aluminum heat sink, yet remove the same amount of heat.

2. Benefit to the DOE's Mission

This work directly benefits the DOE Office of Transportation Technologies and the programs they are funding at ORNL. The study of the interface thermal resistance is of paramount importance to the DOE programs funded to evaluate the graphite foam as a heat transfer medium for power electronics and automotive radiators.

3. Project Objectives and Work Plan

This project is a Phase II SBIR from the MDA in which ORNL is a subcontractor to Materials Resources, Inc. Phase I demonstrated a bonding technique for graphite foam and the Phase II objective has been to demonstrate active solder joined Gr-foam core heat exchangers technology. The work continued to develop joining processes compatible between Gr-foams, fabrication methods that apply to device manufacture, techniques for heat exchanger core configurations and to characterize the performance fabricated graphite thermal management devices.

The Phase II project consisted of:

- Developing active solder joining & fabrication methods, particularly those specific to graphite foam, especially for use in heat exchangers.
- Characterizing active solder/Gr-foam joints as a function of materials and processing methods.
- Conducting thermal performance testing of active solder / Gr-foam joints and comparing them to alternatively joined Gr-foams.
- Conducting more comprehensive thermal and environmental testing of active solder joined Gr-foams.
- Developing methods to fabricate Gr-foam thermal management devices jointly with collaborative partners, Poco Graphite and Thermacore.
- Making thermal management device demonstrator applications.
- Conducting demonstrator performance testing in collaboration with partners.
- Developing commercial scale-up plans with partners.

Technical Work Plan

Phase II work plan had eight (5) distinct tasks:

- Task 1.0 Joining Development
- Task 2.0 Thermal Modeling & Testing
- Task 3.0 Chip Scale Packages
- Task 4.0 Direct Chip Cooling
- Task 5.0 IGBT Package Cooling

4. Results

4.1. Task 1.0 Joining Development

In this task, MRi investigated bonding procedures aimed at various configurations of joints and different types of carbon foam. Both Poco Graphite's PocoFoam and HTC (high thermal conductivity) foam have been used in these experiments, in support of the growing interest in porous graphite for heat exchangers. Evaluations of joint structures and strengths, with varying process conditions, have been performed.

4.1.1. Thermal-Mechanical Testing

In order to determine the longer-range bond integrity between graphite foams with different substrates and different bonding methods, several batches of samples have been subjected to thermal cycling (from negative 40°C to +90°C, under a controlled atmosphere) at Thermacore. After each set of thermal cycles, the samples have been measured for thermal resistance, and any significant changes were documented.

However, the samples all received in excess of 1000 cycles, many of them more than 1500 cycles. As this number exceeds the typical life expectancy for a desktop computer, Thermacore will not be cycling the S-Bonded samples any more, being content that if they were to fail, they would have done so already. However, as the conductive epoxy-joined parts have only seen 600-700 cycles, these will continue cycling for the next few months whenever possible to accumulate at least 1000 total thermal cycles.

Upon removal from thermal cycling, parts will be tested for thermal resistance at least once more before the end of the project, in late spring of 2004. There are already sufficient data to suggest that the approximately 2”x 3” size graphite foam and HTC foam coupons do not experience any significant bond degradation with thermal cycling, under these temperature conditions, for most substrates, as discussed in earlier Quarterly Reports.

Other thermal cycling samples have also been made with aluminum bases and either Poco Foam or HTC foam. These samples were bonded with two different conductive epoxy types as well, and were made to compare with the S-Bonded thermal cycling test samples at Thermacore. These bases had slightly different dimensions from most of the S-Bonded samples, but are still thought to be a legitimate comparator for the S-Bonded samples. When thermal cycling resumes, the epoxy joined samples will be added to the existing sample array and tested alongside the S-Bonded samples.

4.1.2. Reflow Testing

The objective of the reflow testing has been to establish a method to S-Bond® join graphite foam, aluminum and/or copper to one another without mechanical agitation. Reflow joining is defined in this investigation’s case as joining with the S-Bond® filler metal placed in the joint and heated to the reflow temperature without mechanical agitation.

It was found that for joining multi-level stacks of graphite foam and aluminum plates, such as in fin-plate heat exchangers, mechanical agitation would not be practical and/or would not provide sufficiently complete bonding. As such, a development plan has been carried on under this Phase II research to understand the ways in which the molten S-Bond® alloy 220 could be reflowed without mechanical agitation (such as sliding or ultrasonics). In earlier parts of this investigation and in a parallel MDA Phase II contract, it had been found that S-Bond® could be successfully reflow joined at temperatures above 800°C, in high vacuum. The current development has been designed to investigate whether composition or process changes could be made to the S-Bond® joining procedures that would permit in air or “protective gas atmosphere”

S-Bond® joining at temperatures below 550°C, the minimum solidus temperature for many aluminum alloys.

The investigation has been conducted in two parts. One part centered on detailed analysis of the surface chemistries of S-Bond® Alloy 220 as it melts, comparing it to conventional Sn-Ag solders and other composition variations. The other part of the investigation has been aimed a heating/atmosphere process changes that would permit S-Bond® reflow joining. The issue that limits direct reflow joining of S-Bond® to aluminum and copper alloys (typical metals used in heat exchangers) is the fact that a tenacious oxide film forms on the molten S-Bond® alloy when exposed to air at high temperatures, keeping the nascent, active filler metal from being in direct contact with the underlying aluminum or copper alloys. Mechanical agitation has been used to break up these films in the manual joining process. In reflow joining, however, the process relies upon atmosphere interaction and other chemical processes to reduce the oxide film that forms on the S-Bond® 220 alloy and thus permit nascent, molten S-Bond® filler to contact to the aluminum surfaces.

Lehigh University has been contracted to study the surface chemistries of the melting S-Bond® alloy under vacuum and simulate "air" environments. The Auger analysis was conducted from R.T to 600°C, to enable the measurements of the surface oxide films as the S-Bond® filler metal melted. It was discovered that the gallium (Ga) in S-Bond® 220 protects the Sn-Ag matrix from oxidizing. Later in the melting process, over 250°C, the cerium (Ce) has been determined to come to the surface of the melt, again protecting the Sn-Ag from oxidizing too deeply, in effect putting a tenacious but thin oxide layer that normally has to be broken by mechanical means. Up to 500°C, despite the liquidus temperature being 233°C, the Ce oxide-based film kept the molten alloy encased. Above 500°C the Ti migrated to the surface, but the Ce oxide was not reduced at temperatures up to 600°C.

Experiments on aluminum, copper and stainless steel were carried out. It was found that the copper alloy substrate test had reflowed and joined very well to the copper. Upon evaluation of the surface chemistry for the copper substrate, it was observed that a peak in the Cu spectrum occurred as 500°C was approached. This led to the conclusion that Cu interdiffusion into the S-Bond® and along the surfaces of the S-Bond® powder particles was playing a role in reducing the Ce-based oxide film and permitting the nascent S-Bond® Alloy 220 to contact and adhere to the underlying Cu substrate. Surface analysis is continuing and will be conducted under other H_2 rich atmospheres up to 600°C.

The Cu influence on the wetting behavior of S-Bond® Alloy 220 has been taken to the processing level and joining tests have been conducted with copper-modified S-Bond® Alloy 220 fillers. MRi has made 0.5, 1.0 and 2.0 weight percent alloys and we are preparing them for joining tests. MRi has also conducted evaluations of Cu modified S-Bond® 220 powder/pastes. In these compositions, Cu powders were added, up to 2.0 wt%. The reflow joining trials with the Cu-modified S-Bond® 220 pastes worked very well in reflow joining aluminum and copper alloys. MRi is now focusing on Cu additions to S-Bond® 220 based alloys as a way to successfully conduct reflow joining of Gr-foams to Al and copper based materials for assembly into heat exchanger cores. Additional testing is underway.

Task 1.0 Joining Development / Progress & Results to Date:

- Thermal cycling in these conditions appears to have a minimal affect on the thermal properties.
- Investigations into reflow joining using S-Bond® Alloy 220 filler are underway, centering on surface analysis during melting and processing variations. However, it appears that this technique results in the more consistent bond.
- Surface analysis being conducted with Lehigh University has shown the evolution of elements and oxides that protect the Sn-Ag during melting.
- Surface analysis has also shown the Cu diffusing from Cu substrates permits the S-Bond® 220 fillers to wet the base materials via reflow techniques from 500 – 520°C.
- MRi has tested Cu-powder additions to S-Bond® 220 pastes and they have led to successful reflow joining of aluminum and copper.

4.2. Task 2.0 Thermal Modeling & Testing

4.2.1. Thermal Modeling

Heat-transfer modeling and interface heat transfer and corrosion investigations have been mainly conducted under subcontract to ORNL. A flow rig test was used to test the variability of heat transfer properties of the various Gr-foam-material joints, to conduct corrosion investigations, and to create and validate thermal models for the various structures and bond interfaces. The flow rig had capabilities for both air and water cooling, allowing ORNL to work on graphite foam bulk thermal properties & design concepts, bond/interface properties, thermal modeling/prediction, and bond/interface corrosion. This work was conducted to develop a thermal model covering graphite foam types (PocoFoam and HTC), different base materials (Al, Cu, and Al-Gr), and foam configurations (as-cut, corrugated, and finned), for use by thermal design engineers. With the testing on the necessary samples completed, ORNL completed a report defining and then solving the problem for heat transfer through graphite foam, given some known material properties and fluid flow dynamics. This report is attached as Appendix A.

The report discusses the process of using finite element analysis to model heat transfer in a graphite foam heat exchanger, using the known material properties (conductivity, density, etc.) and measurable quantities (fluid and heater temperatures, area, etc.) to predict the outlet water temperature. The report itself covers the details of this analysis.

4.2.2. Thermal diffusivity/conductivity

Cubes of PocoFoam and HTC measuring approximately 5/8” in each dimension were joined to 5/8” square, 1/16” thick aluminum, copper, or aluminum graphite coupons for laser flash diffusivity and thermal conductivity (calculated from the diffusivity) testing at ORNL. Aluminum coupons bonded to HTC and PocoFoam with two different types of conductive epoxy, provided directly by Poco Graphite, were also tested at ORNL, for comparison to data for the S-Bonded samples. Results of these tests are shown in Figures 1 and 2.

It should be noted that recent ORNL research has suggested that the bulk conductivities of PocoFoam and HTC Foam may not be as high as the reported 130 and 245 W/mK, respectively. Samples of non-bonded PocoFoam and HTC foam from the batches of material used for these tests were sent to ORNL to measure the bulk thermal conductivity of these coupons, for comparison to the reported values, Figure 3.

Progress & Results to Date

- Laser diffusivity/conductivity tests were completed.
- The epoxy bonded samples generally did not perform as well as the S-Bonded samples.
- The reflow technique appears to give the best bond, but inconclusive.
- PocoFoam® exhibited the highest thermal diffusivities conductivities compared to that of the Poco HTC®. However, the Poco HTC appeared to exhibit the highest thermal conductivities.

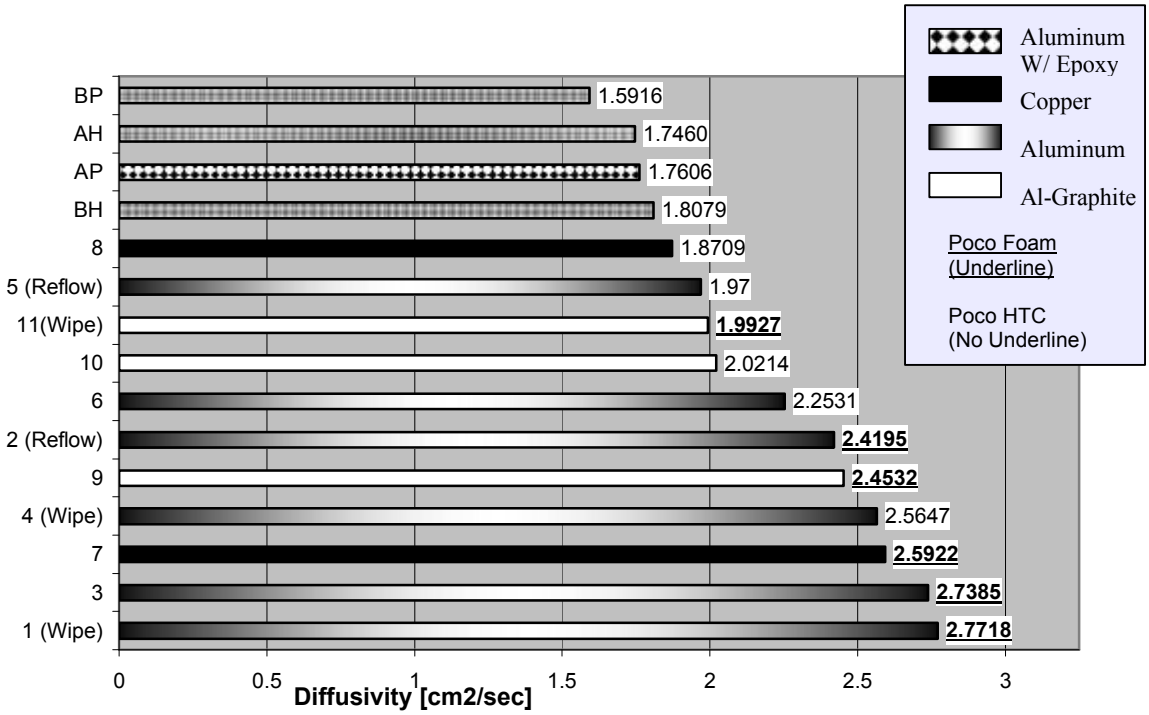

Figure 1. Average Measured Thermal Diffusivity of PocoFoam® and PocoHTC® samples bonded to various substrates.

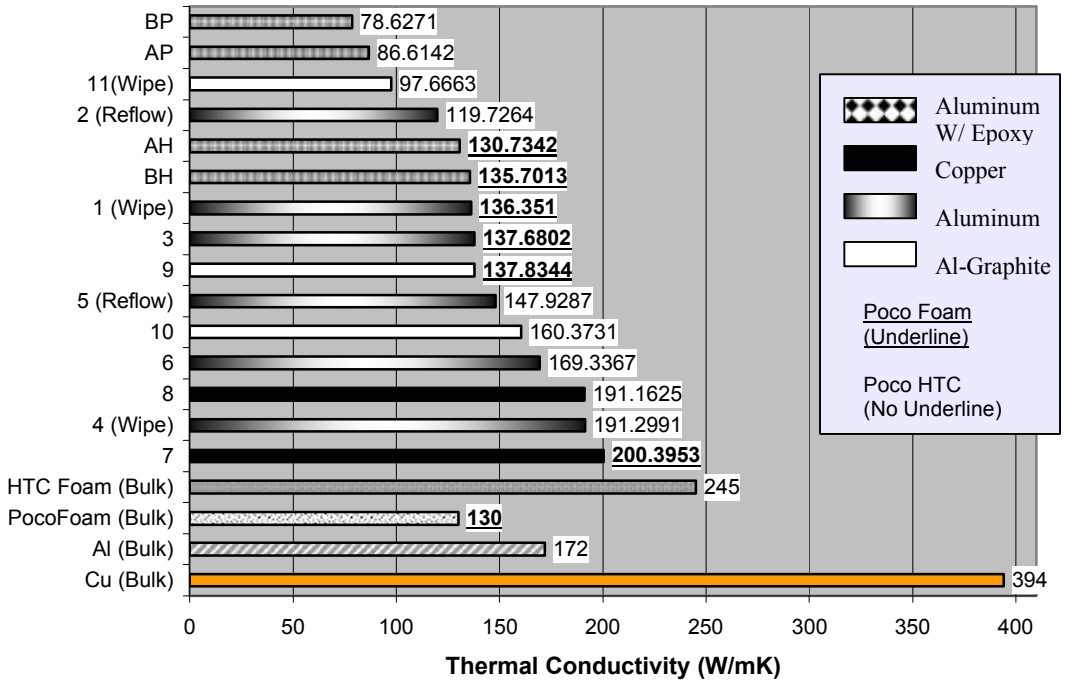

Figure 2. Average Measured Thermal Conductivity of PocoFoam® and PocoHTC® samples bonded to various substrates.

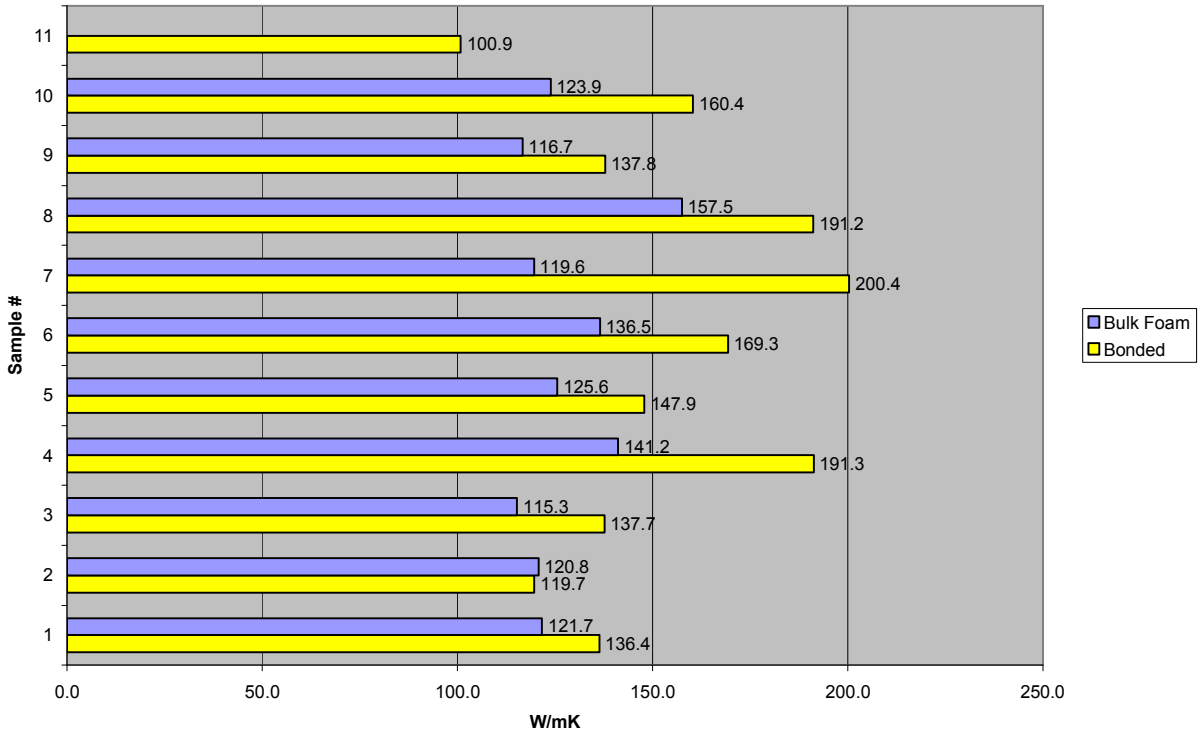

Figure 3. Average Measured Thermal Conductivity of PocoFoam® samples bonded to aluminum substrates before and after bonding.

4.3. Task 3.0 Chip Scale Packages

Thermacore supplies fin-plate type heat exchangers for consumer and workstation computers, such as that for the Pentium IV processor chip package. The base typically consists of a rectangular solid base of copper or aluminum, or a flat rectangular heat pipe for improved performance. The base spreads heat from a concentrated heat source, i.e. the chip package, to the bases of the fins, which are mounted on the opposite side, with air forced through the fin array by a fan at constant power. This task aimed to compare aluminum folded fins with graphite foam, either as a fin or another type of structure compatible with air flow cooling.

Multiple samples of different bonding methods, base materials and foam types were assembled of both the 423-pin (Figure 4) and 478-pin (Figure 5) heat sinks were tested and the are shown in Figures 6-9. Note that 423 and 478 refer to the type of integrated circuit that the heat sink was designed to cool.

A copper-based, aluminum finned, 478-pin heatsink was joined with S-Bond 220 and labeled (NRF), to be tested in the same manner as the foam samples were and thereby produce a direct comparison of the graphite foam fins to the conventional aluminum fins. Up to this point, there were reference standards for comparison, but these were made entirely from either aluminum or

copper, and therefore there was no direct comparison of aluminum fins on a copper base with graphite foam fins on a copper base.

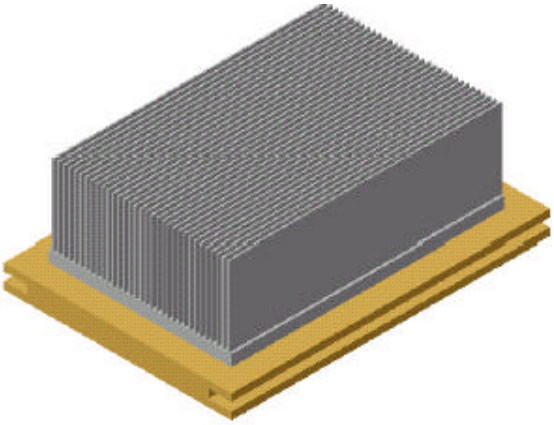

Figure 4. Design for 423-pin graphite finned foam heat sink.

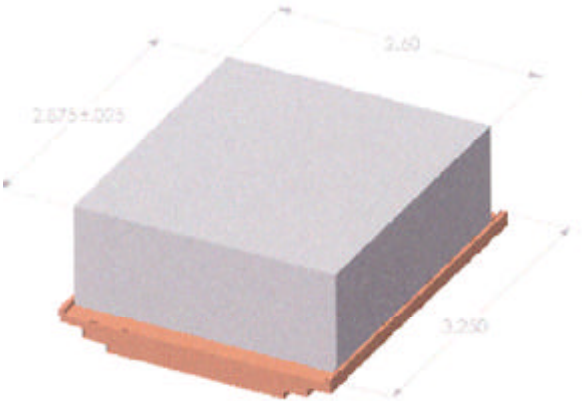

Figure 5. Design for 478-pin graphite finned foam heat sink.

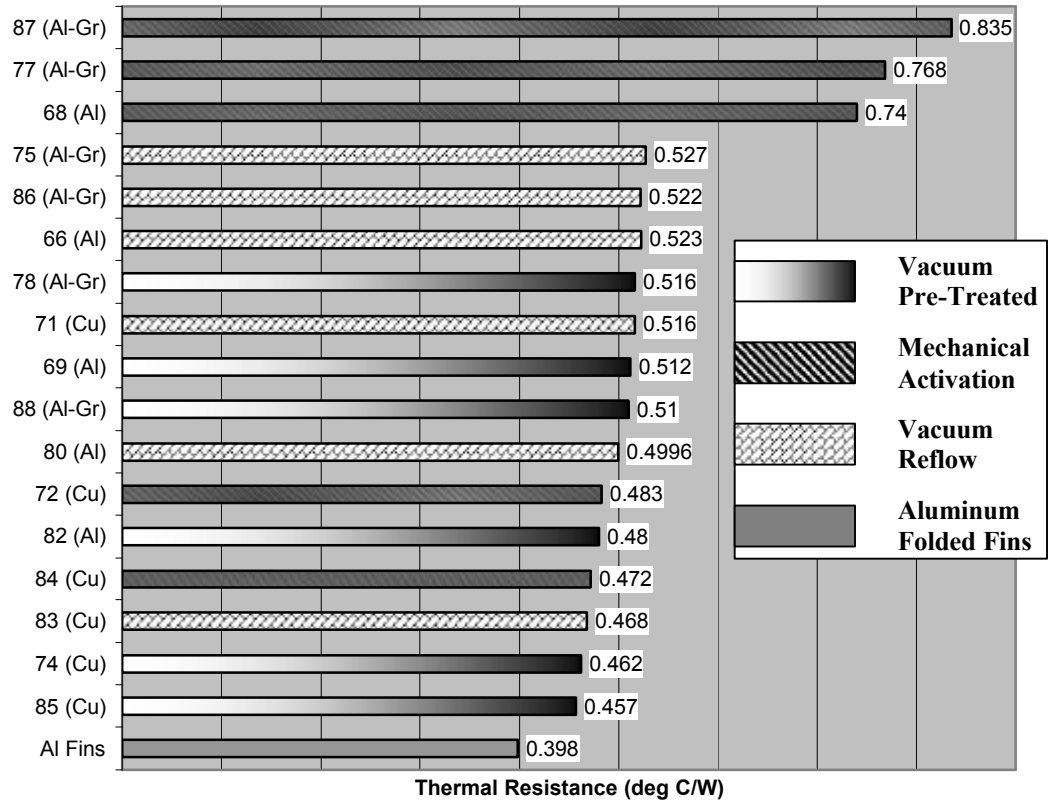

Figure 6. 423-Cooling Package Thermal Resistance Data

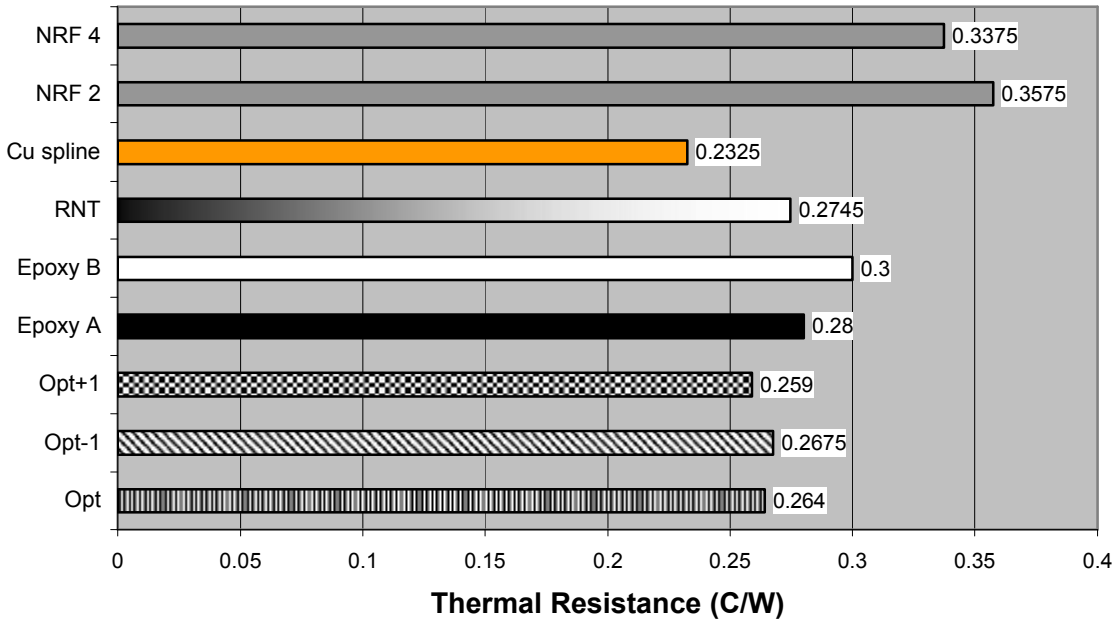

Figure 7. 478-Pin Chip Cooler Summary

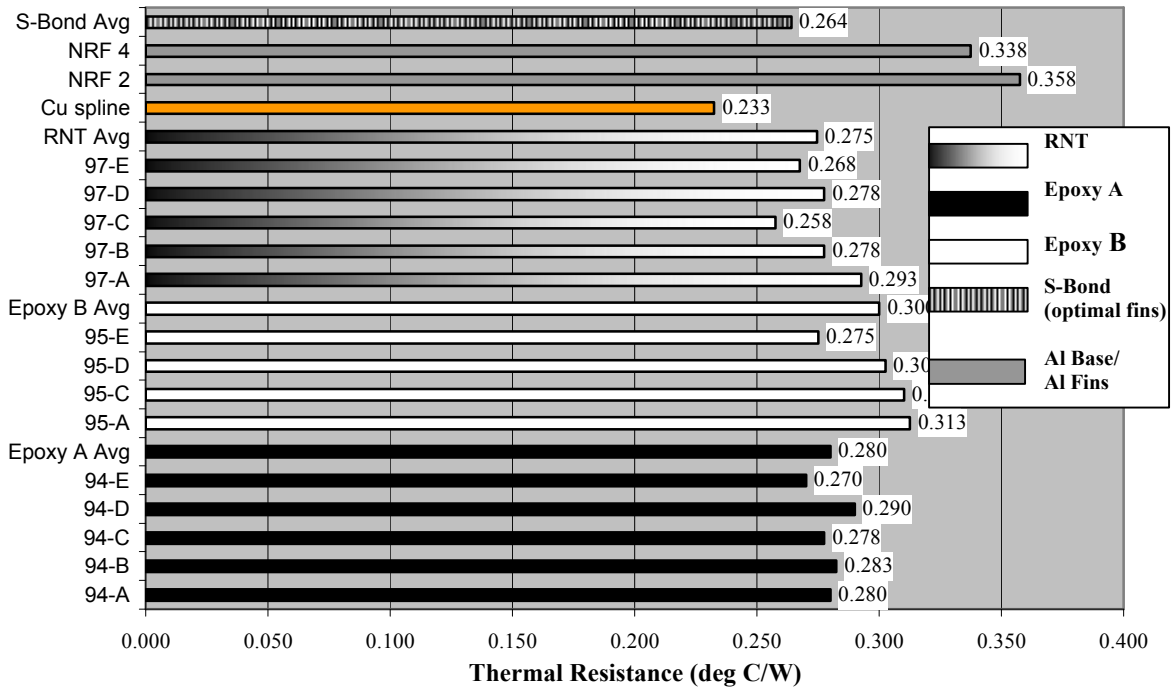

Figure 8. 478-Pin Chip Cooler Bonding Effects

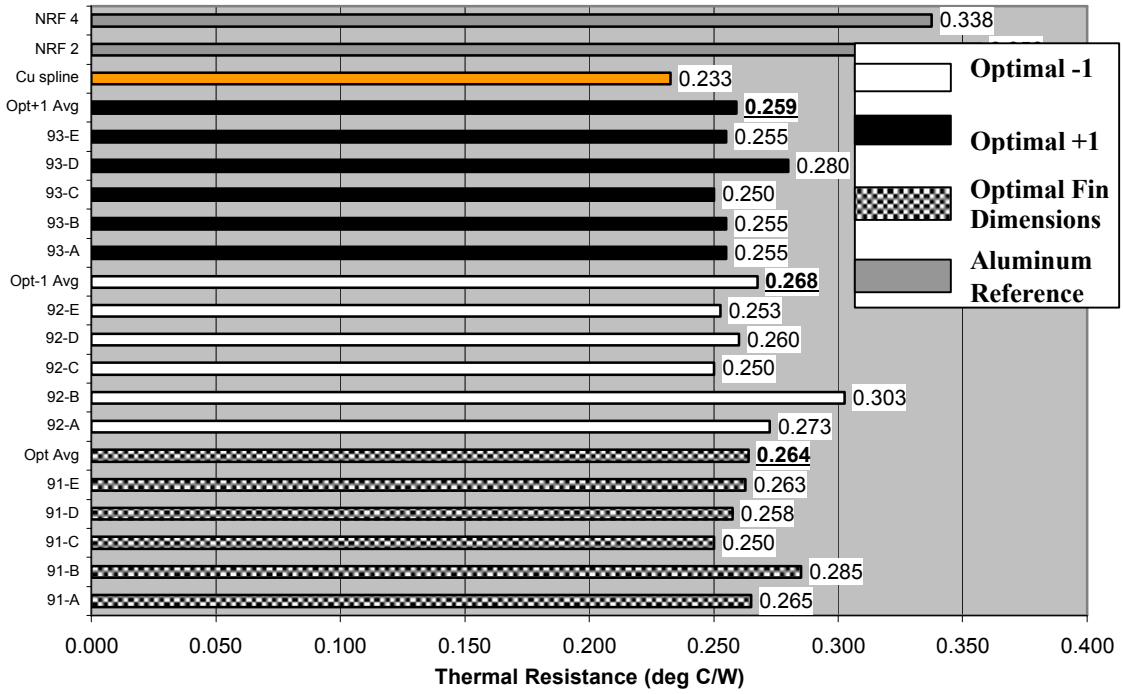

Figure 9. 478-Pin Fin Dimension Variation Effects

4.4. Evaporative Cooling

Thermacore has joined in the effort as the primary developer for this application, which has been re-focused to concentrate on an evaporative cooler for direct chip cooling. Thermacore's database contains a great deal of information on evaporative coolers, especially of the design shown in Figure 10, which is a wick material, bonded to a heat spreader, submerged in an evaporative liquid, and enclosed in a sealed chamber. The heat created by the chip (bonded to the other side of the heat spreader) is dissipated into the conductive wick and transferred to the liquid, which evaporates and then condenses on the outer surfaces of the chamber, transferring the heat from the chip to the external air, without the use of a fan. In this model, the graphite foam would act as a wick to draw away heated coolant, as in a heat-pipe.

Three samples, as shown in Figure 10, were made for testing HTC foam in such a setup, and another three samples were made for testing Poco foam. In addition, two more types of graphite foam (designated Conoco and AR-9) were also used in such assemblies (three samples each), and were sent to Thermacore for testing. The Conoco and AR-9 foams are comparable in density to the HTC foam but have much finer pore sizes, and therefore may be more suitable for this 'wicking' application than either PocoFoam or HTC-foam. The samples consist of a small copper endcap, S-Bonded to a piece of foam, which was machined to match the diameter of the copper endcap. The three assembled samples for each type of foam were milled to thicknesses of 1 mm, 2 mm and 3 mm, soldered together and then tested in the simulated evaporative cooler. In addition, a sintered copper heat pipe is also being tested in tandem with the graphite foam samples for a baseline comparison.

It was reported by ORNL that methanol wets the foam well, whereas water does not, therefore methanol is being used for the first sets of test samples. Subsequent test sets will likely be done with water and some wetting agent, rather than with FC-72 or FC-87 (fluoro-carbon refrigerants), as originally planned.

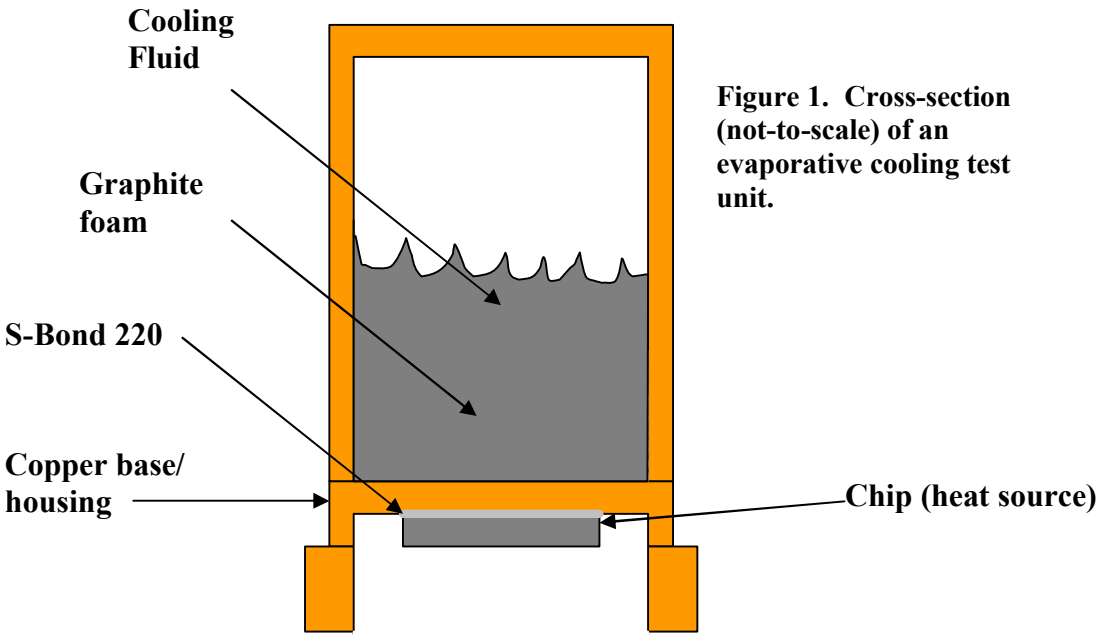

Figure 1. Cross-section (not-to-scale) of an evaporative cooling test unit.

Figure 10. Heat Pipe Design

Because it was reported by ORNL that methanol wets the foam well, this was used for the first sets of test samples. Subsequent sets of tests will likely be done with water and some wetting agent, rather than with FC-72 or FC-87 (fluoro-carbon refrigerants), as originally planned. The twelve samples were assembled and tested, and the results to date are shown in Figures 11 and 12, along with the results of the sintered copper heat pipe. These results are not fully understood yet, and must be analyzed further before any conclusions can be presented regarding them. Figure 11 shows that the thermal resistance exhibits an apparent decrease as the thickness of the wick is increased from 1mm, which contradicts expectations. That is, a thicker wick, because it offers more material through which heat must travel, should yield a higher thermal resistance, which is generally not the case for these parts. For two- and three-millimeter wick thicknesses, there does not appear to be an appreciable change in thermal resistance, though at some critical thickness, the thermal resistance would be expected to increase again. The general consistency of the 2- and 3-mm thermal resistance is likely an indication of the excellent conductivity of the graphite foams.

One possibility for the downward trend may be that the S-Bond alloy within the pores on the bonded side of the foam creates additional mass through which the heat must pass, thereby increasing the thermal resistance for thinner wicks. As the wick thickness is increased, the comparatively lower-conductivity SBond material (48 W/mK) becomes less of a percentage of the total mass, and therefore less of a factor in the thermal resistance of the couple. The higher conductivity foam (110-200 W/mK) becomes the primary factor in the thermal resistance of the system over a certain thickness.

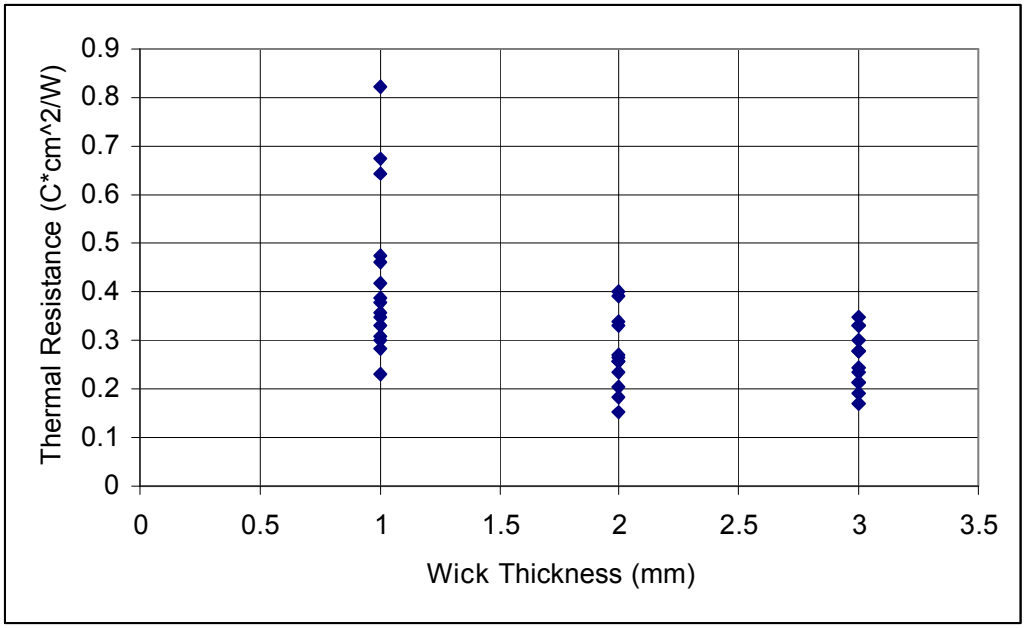

Figure 11. Thermal Resistance of Evaporators vs. Wick Thickness

The next set of data would be expected to show that the thermal resistance increases as the heater input power is increased, but instead no clear trend can be discerned from the available data, shown in Figure 12. The sintered copper evaporator seems generally to have lower thermal resistance at lower heater power, but to come back into the range of the graphite test samples at higher power, as shown in Figure 12. There is a lot of scatter in the data, which have been acquired from testing with low-boiling point methanol, necessitating lower temperature results. As testing is planned with higher-boiling water, it is hoped that these higher temperature tests will help eliminate some of this scatter and clarify the capabilities of S-Bond 220 and graphite foam in evaporative cooling applications. In addition, higher-temperature testing may help to discern how well S-Bonded graphite foams compare to sintered copper wicks for higher-heat flux applications.

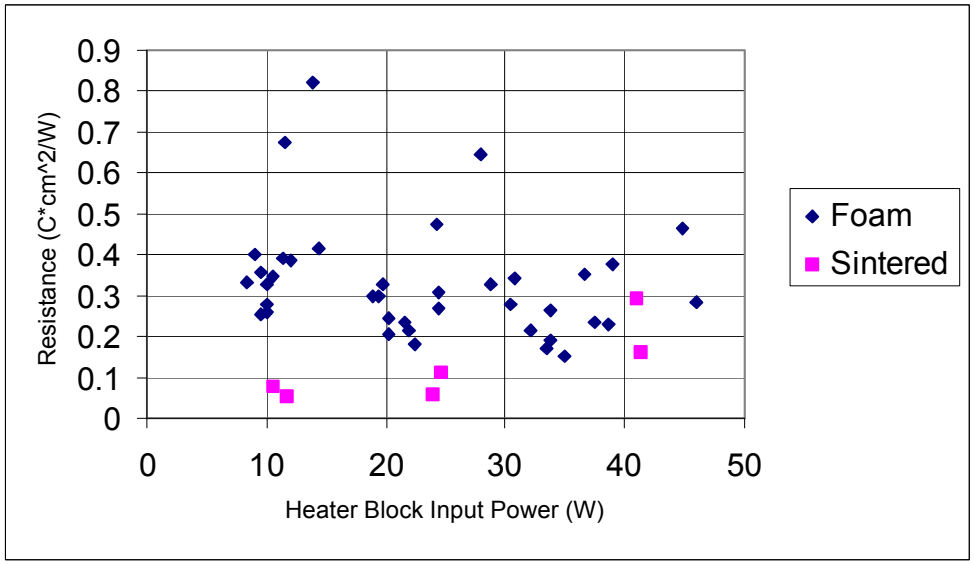

Figure 12. Thermal Resistance of Evaporators vs. Base Heater Power

One issue to be addressed in order for evaporative cooling to work is the environmental compatibility of S-Bond alloy(s) with the cooling liquid(s) used in an evaporative cooling system. This was done by prewetting thin samples of annealed copper strip with S-Bond 220 and then enclosing them in an environmental chamber with conditions similar to that of an evaporative cooler (temperature, pressure, humidity, cooling fluid, etc.), see Figure 13. In addition, similar samples were made to incorporate the foam material, to see how this would affect the results, if at all. Any corrosion or other deterioration of the system is then documented, generally by a temperature increase or by the evolution of any gases within the chamber. Seven samples with only S-Bond 220 and seven with both S-Bond 220 and graphite foam were submitted for testing.

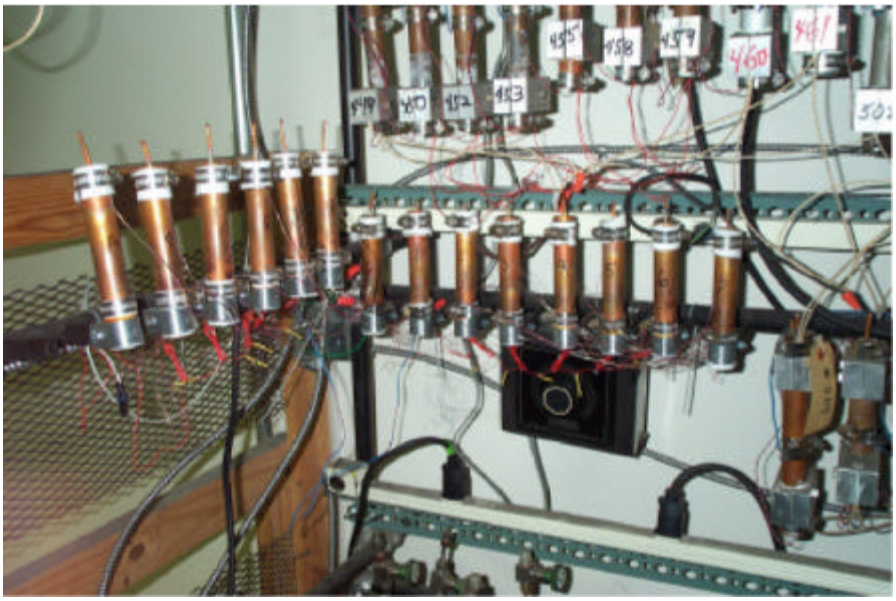

Figure 13. Extended life testing of foam heat pipes.

Environmental compatibility samples were made at MRi and submitted to Thermacore for assembly. Initial data from these tests were inconsistent. Initial measurements of ΔT (between the tops and bottoms of the test units) and plots of these vs. Time seemed to indicate that the S-Bond only samples were producing gases and that the S-Bond samples with graphite foam attached to them were producing no gas at all.

Conversely, cutting the test temperature in half and measuring the ratio of ΔT/Power seemed to indicate the exact opposite result, that the S-Bond/graphite samples were evolving gases and that the S-Bond only samples were not. That is, analysis of the samples in two different manners yielded conflicting and opposite results.

Additional testing is still underway in hopes of bringing the sets of data into agreement with each other, though no new data were available for this report.

After the last round of data was taken from these samples, the power was cut in half and the temperature differences between the tops and bottoms of each of the 14 samples were re-measured. Decreasing the heater power should theoretically yield a linear decrease in the temperature difference (ΔT), if there are no gases evolving inside the evaporator. That is, cutting the power in half should also cut the ΔT in half, if the materials in the system are environmentally compatible. The ratio of (ΔT1/Power1)/ (ΔT½/Power½) therefore should be approximately equal to 1.0, with no gas evolution inside the chamber, and should be greater than 1 if there is gas evolution, i.e. an environmental incompatibility. The results of these tests are shown in Figure 15.

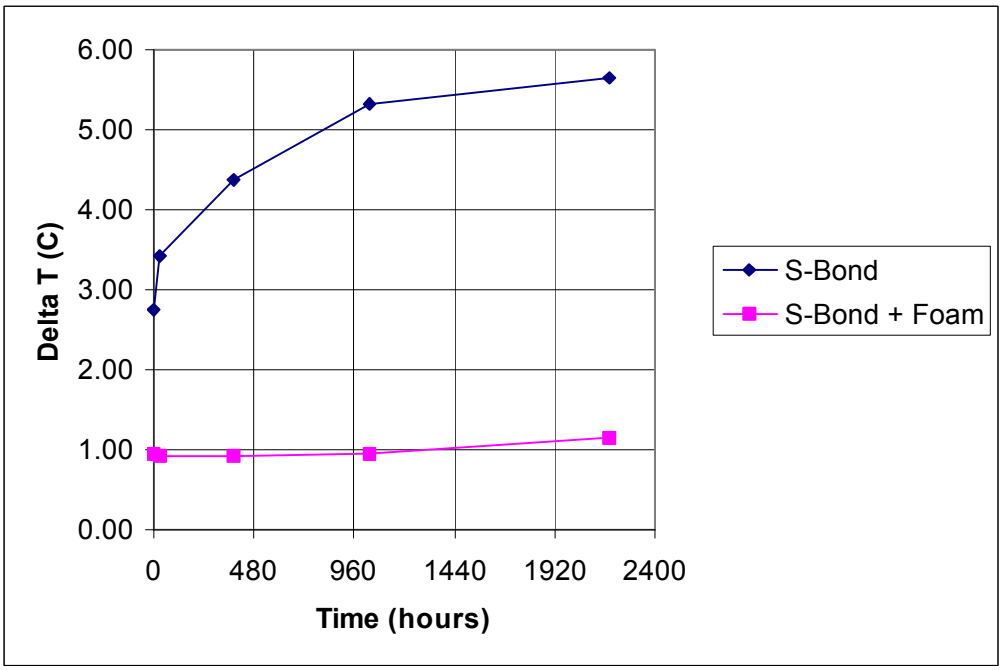

Figure 14. Environmental Compatibility Tests: DT vs. Time

As Figure 15 shows, the samples with S-Bond and PocoFoam generally exhibited a ratio greater than 1.0, indicating gas evolution, while the samples with S-Bond only generally had a ratio less than or equal to 1.0, indicating no gas evolution. These results are the exact opposite of the results gleaned by the ΔT vs. time studies, as shown in Figure 14. These results are as yet inexplicable and it is hoped that additional testing will yield more conclusive data.

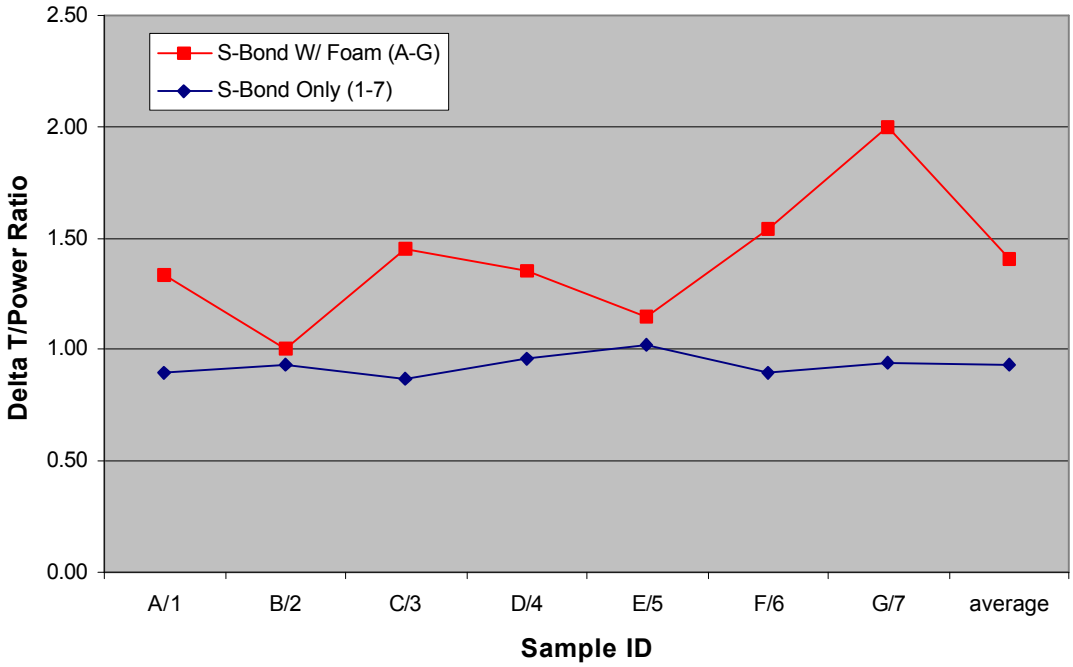

Figure 15. Heater Power Decrease Effects

Progress & Results to Date

- Thermacore tested evaporative chip-coolers with different types of graphite foam and varying thicknesses in a simulator.
- Results were contradictory to standard heat pipe wick material in that as the foam thickness increases, the thermal resistance decreases. This is opposite to traditional wick material.
- Methanol may not be the fluid of choice with S-bond and graphite foam due to some potential environmental degradation.

4.5. Task 5.0 IGBT Package Cooling

Thermacore has selected the IGBT style component as a test vehicle for demonstrating scaling from the chip-cooling package (~2" x 3") to larger heat exchangers for large area, medium power density cooling (up to 8" x 12"). ORNL posited the idea that this application would help to "bridge the gap" for demonstrating S-Bond joining and graphite foam cooling capabilities, as shown in Figure 2. To this point, the contract had covered relatively small, low-power density applications (like the Pentium-style chip cooler) and very-high power density applications, which typically only encompass a very small area, like the aforementioned evaporative cooler. This Task will allow MRi and its partners to show the capabilities of S-Bond and Graphite foam in a larger-area, moderately high power density application (~30 W/in^2), such as the cooling needed for power switching devices, like the IGBT.

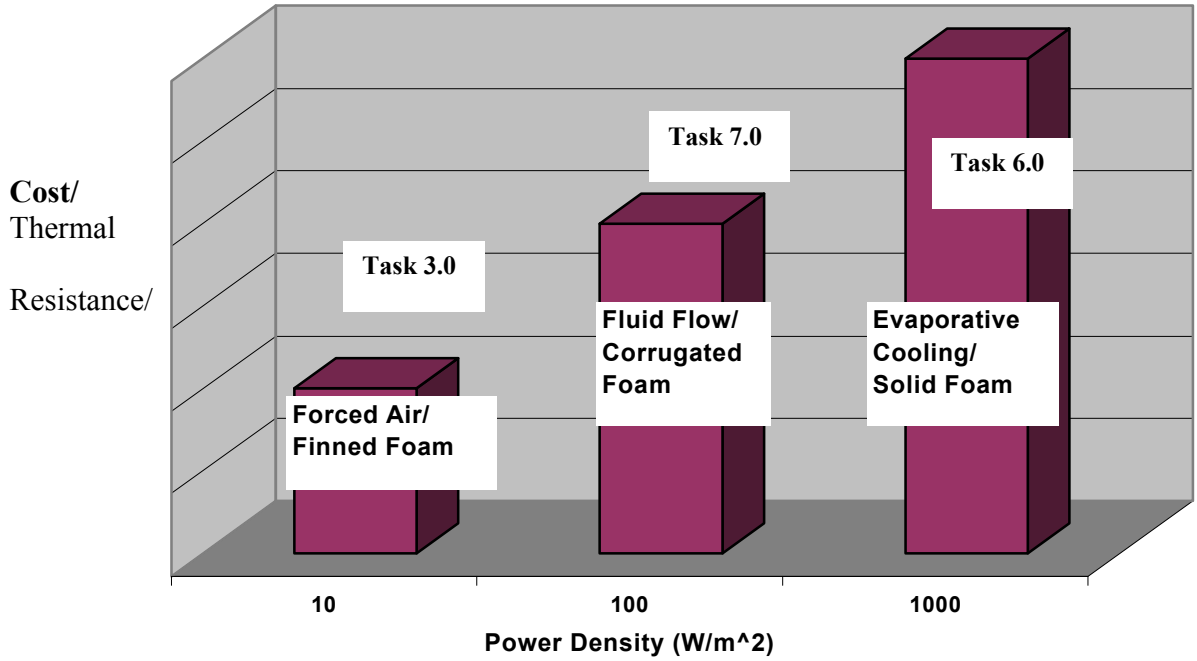

Figure 16. Design Considerations vs power density.

A schematic representation of the test plates is shown in Figures 17-19. This is a similar concept to that originally demonstrated at ORNL. Foam is corrugated in the design shown and bonded to the cold plate. A lid is placed on top of the foam such that all fluid is forced to pass through the foam. The fluid enters the manifold and then passes down the channels between the foam webs. The fluid is then forced to turn horizontal and flow through the pores of the foam, where the fluid then leaves the next channel to the exit manifold. In this fashion, the fluid only passes through a short length of foam, thus reducing pressure drops.

Initial tests on the three PocoFoam coldplates were performed first with methanol as a cooling fluid, and later with 50/50 ethylene glycol/water, at flow rates up to 3000 cc/min. These tests and their results were described and discussed below.

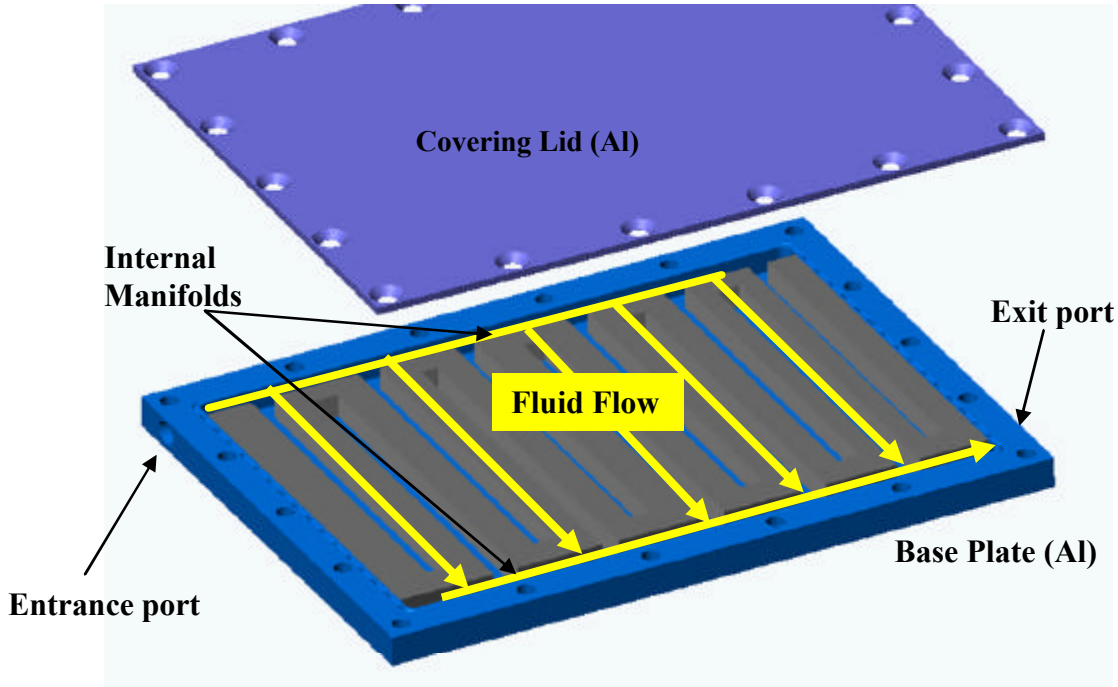

Figure 17. Schematic design of IGBT cooling plate.

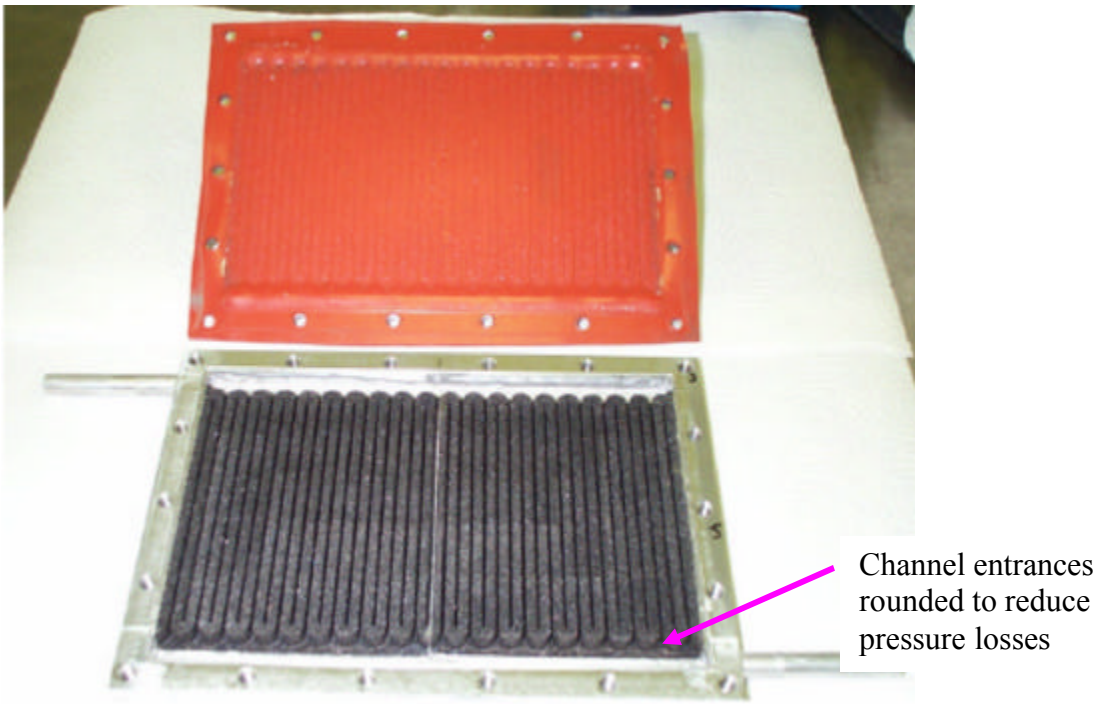

Figure 18. Graphite foam corrugated cold plate with lid.

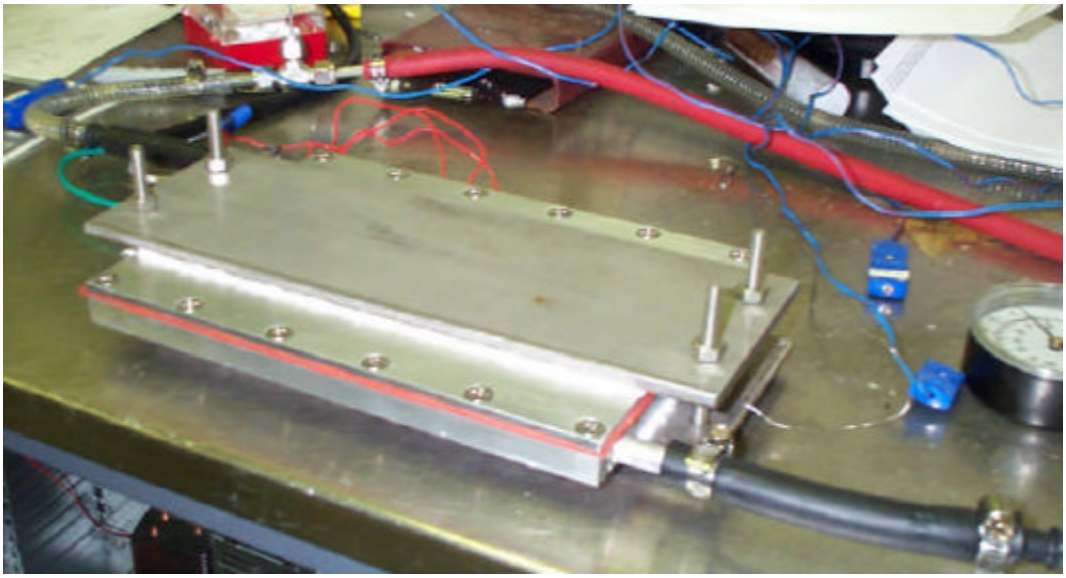

Figure 19. Cold plate test set up.

Testing has been completed for all three coldplates with 50/50 ethylene glycol as well as with water. The results of the 50/50 tests, shown in Figures 20-22, indicate that higher heat input can be reached and cooling maintained effectively with moderate flow rates.

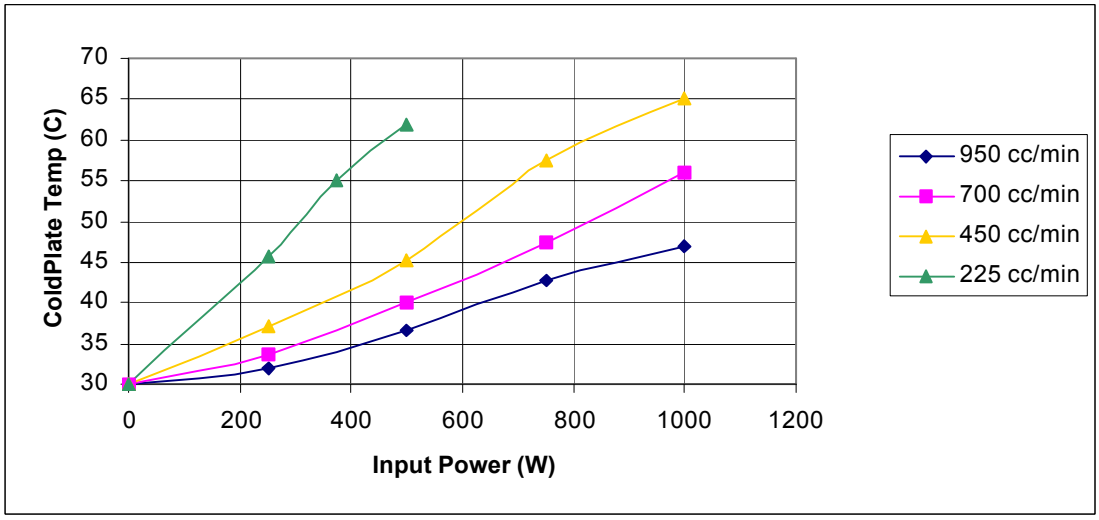

Figure 20 IGBT Coldplate #1 –Water/Glycol

Additional testing has been performed on graphite foam Coldplate #3 with 100% water, first at flow rates up to 1000 cc/min, like the previous tests, and these results are shown in Figure 8. As would be expected, the results of these tests were comparable to the results of the 50/50 tests, in terms of the temperature maintained at the highest flow rates and power input levels.

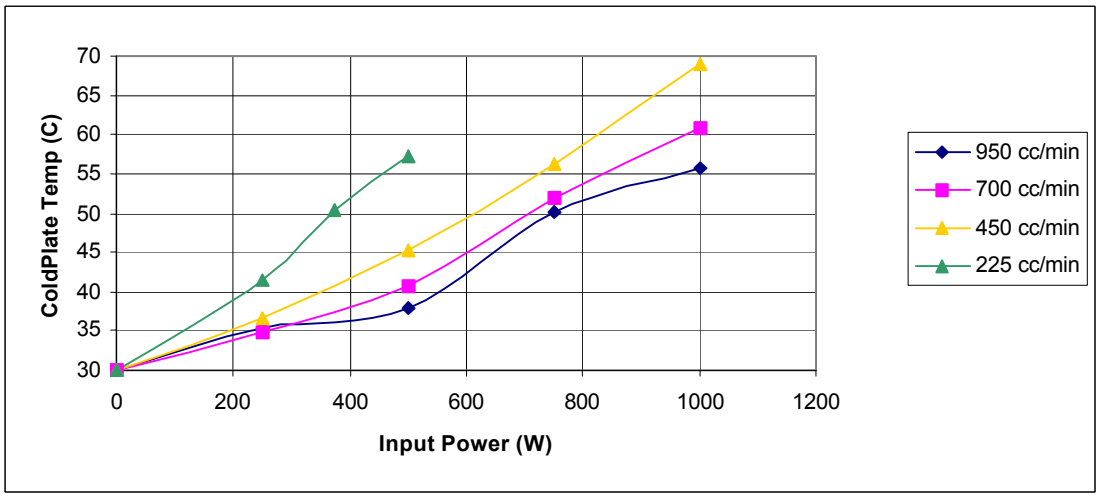

Figure 21 IGBT Coldplate #2 –Water/Glycol

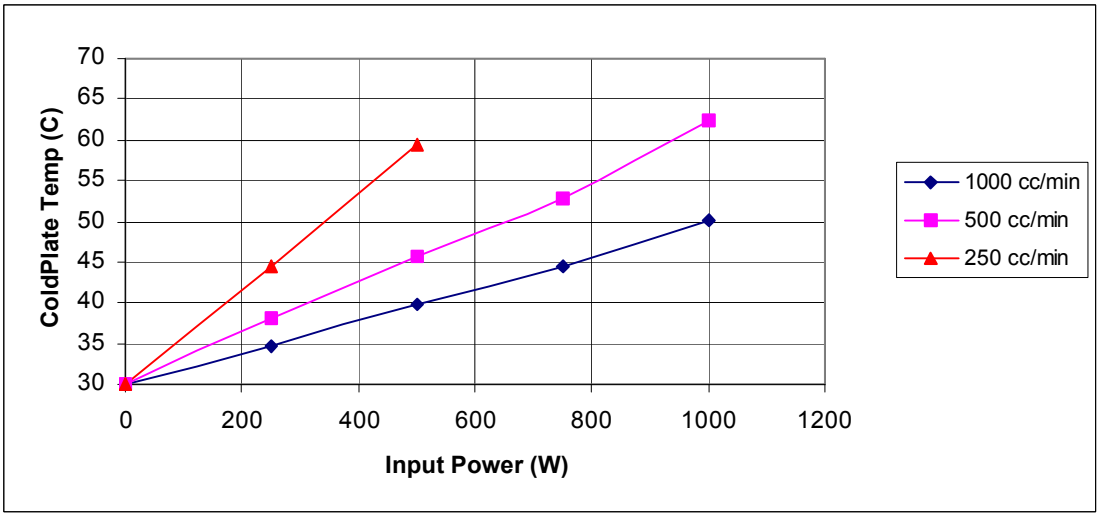

Figure 22 IGBT Coldplate #3 –Water/Glycol

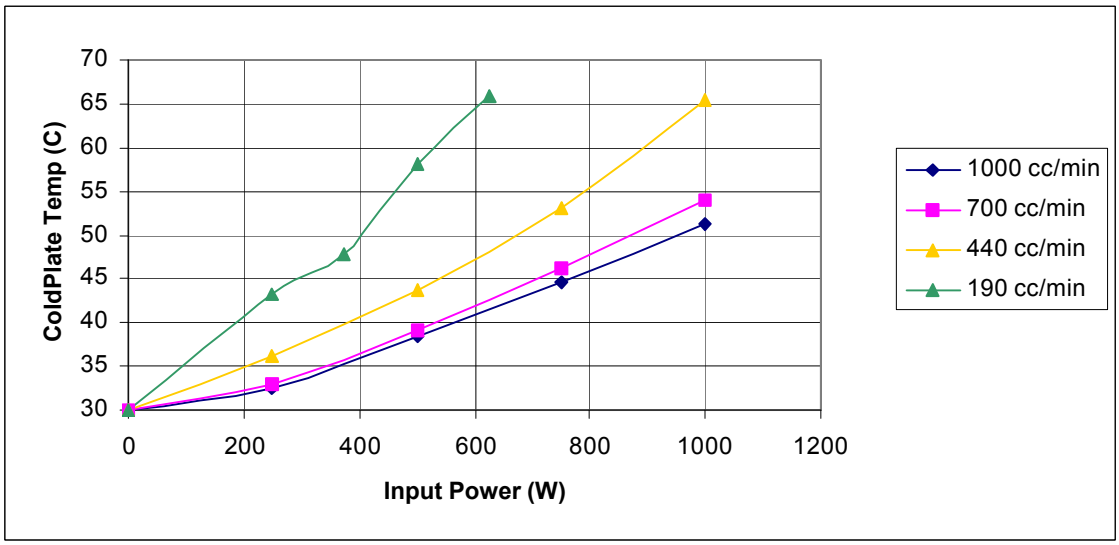

Figure 23 Coldplate #3 – 100% Water

After this, Coldplate #3 was tested with water at flow rates up to nearly 3000 cc/min, at constant heat input of 1000 W. Results at higher flow rates were encouraging, showing a thermal resistance at the highest flow rates of about 0.46 W/mK, lower than originally projected (Figure 24). The other two coldplates are not currently being tested with 100% water in order to prevent corrosion of the aluminum inside the coldplates.

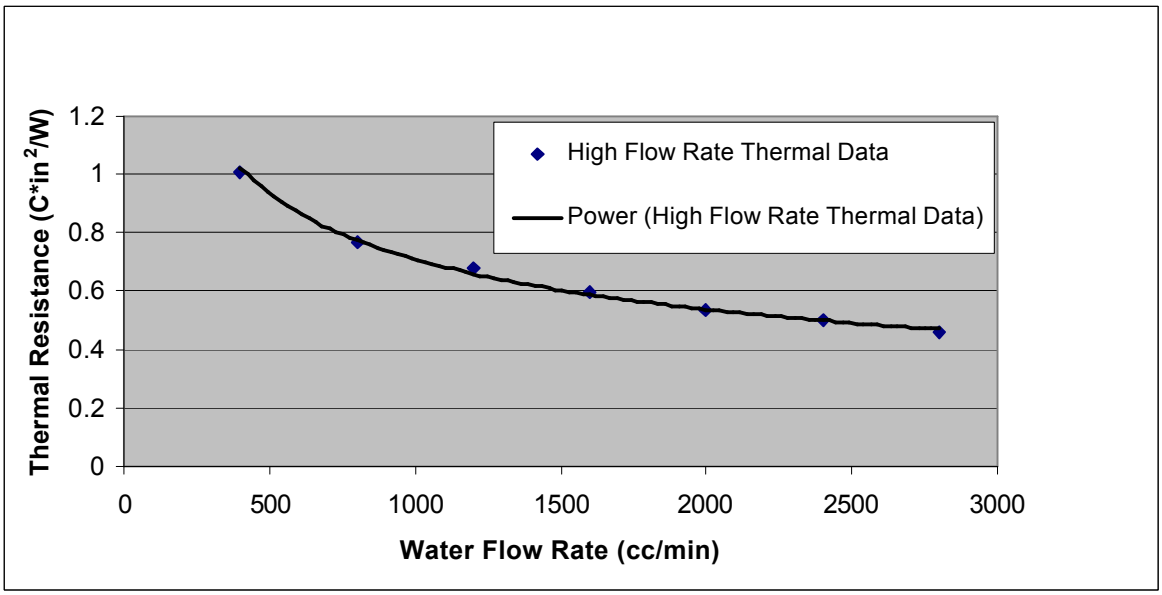

Figure 24 Thermal resistance of Water-Cooled, High-Flow, Al/Gr Foam Coldplate

Pressure drop was originally thought to be a potential problem at higher flow rates, but now appears to be within acceptable limits, and even levels off somewhat at the highest flow rates, see Figure 25. Though the pressure drop did increase more quickly than had been originally projected, the final results at high flow rates were within an acceptable range (~5psi @ 2500 cc/min).

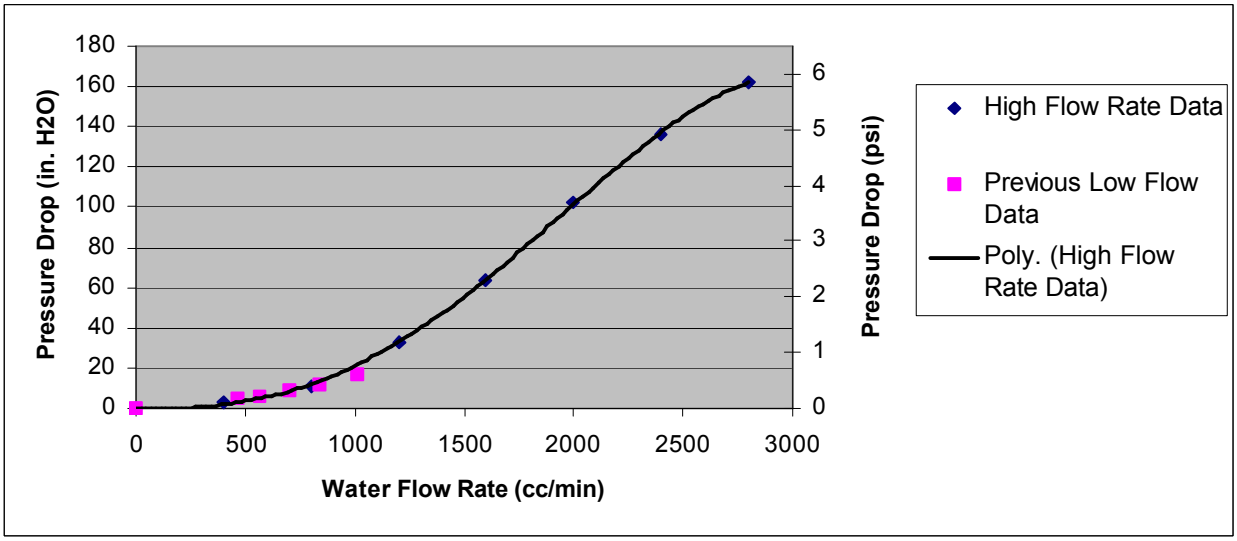

Figure 25 Pressure Drop Effects (100% Water in Al/Gr Foam Coldplate)

To provide a comparison to conventionally available technology, contract partners determined that it would be best to produce a unit to which these S-Bonded, Pocofoam coldplates could be directly compared. This would allow prospective customers to have an immediate idea of how much better PocoFoam performs than aluminum folded fins, if it does at all, as well as any limitations of the technology. Since folded aluminum fins are the conventional cooling technology, it is necessary to demonstrate the extent to which PocoFoam can outperform them, in order to justify its cost.

Thermacore's initial tests on the first of two aluminum folded fin coldplates revealed that the aluminum fins provided a slightly lower pressure drop at most flow rates, approximately 10-20% better than the graphite foam, as shown in Figure 26. However, Thermacore's tests also showed that the graphite foam coldplate provided a significant improvement in thermal resistance, approximately 40% lower, as shown in Figure 26. Similarly, and perhaps more importantly, the data in Figure 26 also indicate that the cooling fluid flow rate can be cut down to 1000 cc/min in the graphite foam coldplate, and approximately the same thermal resistance is achieved as with a flow rate of 3000 cc/min in the aluminum finned coldplate. This means that much less power can be utilized in forcing flow through the coldplate to achieve the same result, and that more effective cooling can be easily accomplished, if necessary. The ratio of pumping power between the graphite foam sink and the aluminum sink is defined as:

$$\frac{\Delta P_{GF} \cdot V_{GF}}{\Delta P_{Al} \cdot V_{Al}} = \frac{0.8 * 1000}{5.5 * 3000} = 0.048 = 5\%$$

Hence, the pumping power with the graphite foam sink is roughly 5% than that with the aluminum sink, yet the same thermal resistance results.

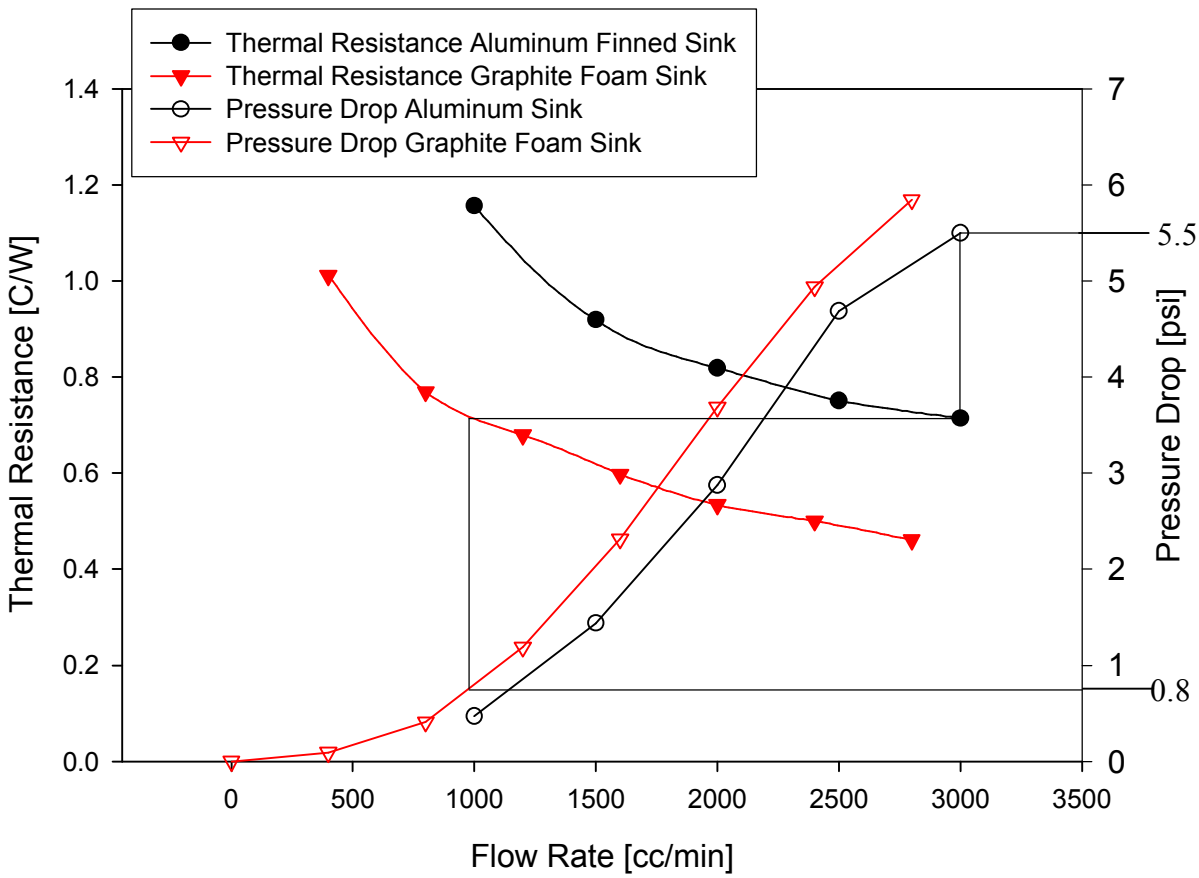

Figure 25. Plot of performance of a graphite foam sink to a folded fin louvered aluminum heat sink.

These are excellent findings:

1) That the graphite foam is capable to provide a significant drop in thermal resistance, at the same flow rate, with only a minor increase in pressure drop.
2) That the graphite foam can provide essentially the same thermal resistance, with a flow rate almost 33% of what is needed in aluminum finned coldplates of the same design. This corresponds to a reduced pressure drop when compared to the aluminum sinks.
    a. For example, in Figure 12, at a thermal resistance of 0.7 C/W, the aluminum sink will require a flow of 3000 cc/min and a pressure drop of 5.5 psi.
    b. Comparitively, the graphite foam sink will only require 1000 cc/min at a pressure drop of 0.8 psi.

This is a remarkable finding.

3) That the graphite foam channels offer a noteworthy weight savings over the aluminum fins.

These facts should serve to encourage thermal management design engineers that PocoFoam and S-Bond are technologies that can open up new markets and new applications, especially in the power switching industry, where large areas of moderately high power density must be cooled effectively. To verify these data, a second aluminum finned coldplate will be tested in water only, and then both coldplates will be tested with the 50/50 water/ethylene glycol mixture, which is a preferred coolant, given that aluminum will begin to corrode with water as a coolant.

Progress & Results to Date

- Thermacore has completed testing of three (3) 8" x 5" aluminum/S-Bond 220/PocoFoam cold plates with two different cooling media (methanol and 50% each water/ethylene glycol) and a one of these plates has also been tested with only water.
- Results of these tests have indicated that the coldplates perform reasonably well, that is, that they are capable of maintaining acceptable coolant operating temperatures with an acceptable level of pressure drop at high flow rates (>1000cc/min).
- Thermacore has tested one of two aluminum-finned, aluminum-based, S-Bonded coldplates for direct comparison of the graphite foam to aluminum fins.
- Results have indicated that the graphite foam offers a significant weight savings and a significant thermal resistance improvement with only a nominal increase in pressure drop, at comparable flow rates. In addition, nearly identical thermal resistance levels can be achieved with approximately 30% of the flow rate necessary for similarly designed aluminum fin coldplates, yielding a required pumping power that is $1/20^{th}$ that of the aluminum plate.

4. Inventions

There were no inventions in this CRADA.

5. Commercialization Potential

Currently, there are potential licenses with Thermacore for cold plates and evaporative cooling designs. There are many other chip cooling potential licenses that are a result of developing a good bonding technique.

6. Plans for Future Collaboration

MRi, Thermacore, and ORNL are discussing options for future collaboration on other proposals to DOD. In addition, there is potential for collaboration in licenses with Thermacore for cooling systems for electronics.

7. Conclusions

The graphite foam was found to outperform aluminum heat sinks when a proper bond was developed. This bond was found to be a wipe/reflow technique developed at MRi. In addition, a cold plate with graphite foam was developed that exhibited similar heat transfer to optimized louvered aluminum fins cold plates, but at $1/20^{th}$ the pumping power. In addition, the weight of the systems made with the graphite foam were significantly lower in weight as well. This is a significant result as reducing pumping power while maintaining heat transfer is the goal of all automotive heat exchanger developers.

8. Acknowledgements

This research was supported through a CRADA with Materials Resources International, MRi, sponsored by the U.S. Department of Energy, under contract DE-AC05-96OR22464 with Oak Ridge National Laboratory managed by UT-Battelle, LLC.

9. Appendix A: Heat Transfer Modeling

8.1. Problem definition:

A block of foam is bonded to an aluminum plate as a heat sink. An electronic device is placed on the top of the aluminum block and dissipates up to 600 Watts into the aluminum plate and then to the carbon foam. The block of foam is mounted in a channel such that either air or water will be forced through the foam as a cooling fluid. Typically, water is the cooling fluid and its inlet temperature is 20C. Figures 1 and 2 illustrate the problem graphically.

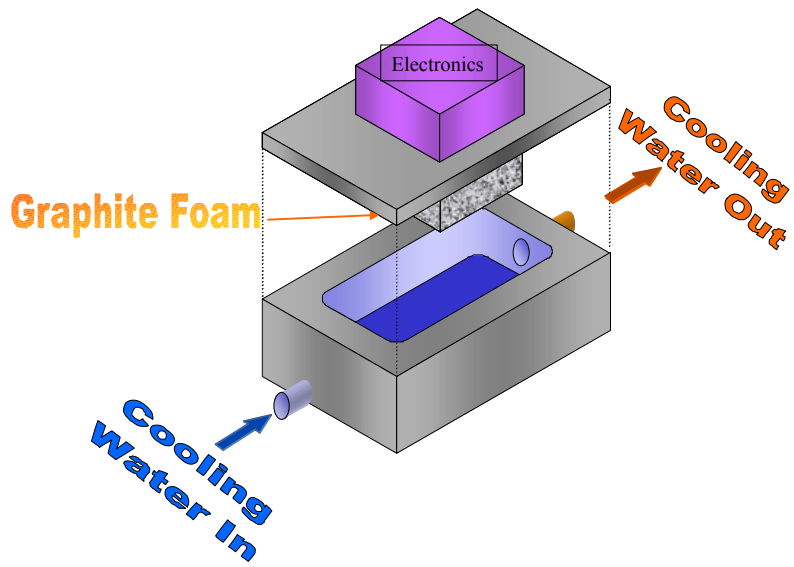

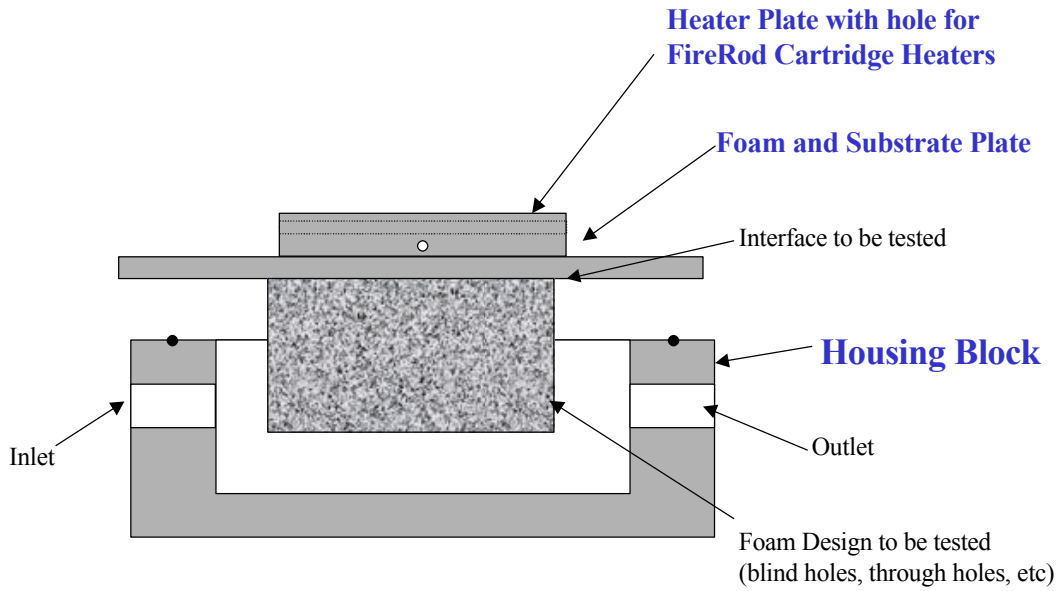

Figure A1. Schematic representation of the design of the foam as a cooling heat sink.

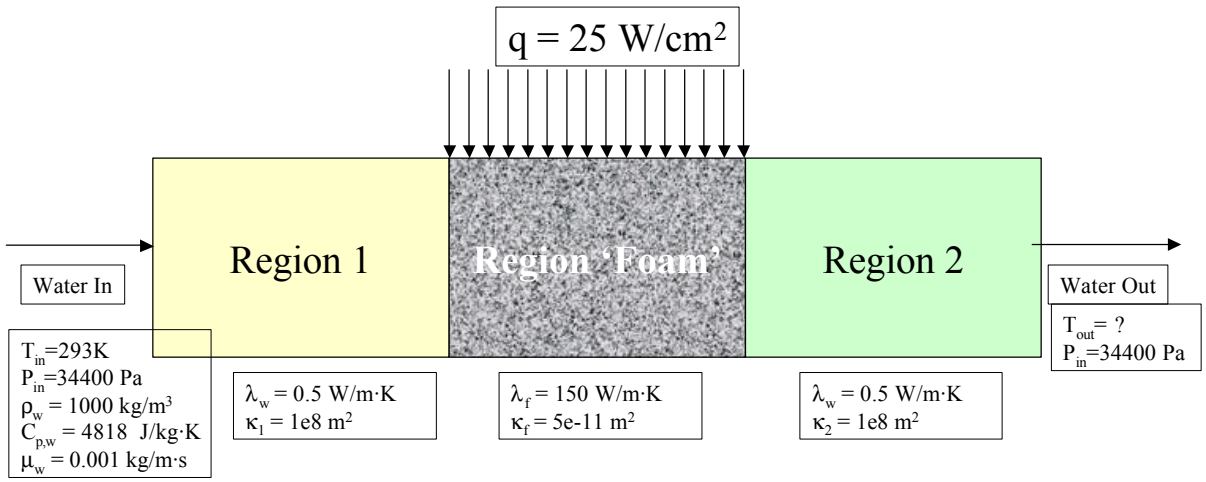

Figure A2. Model geometry for problem descriptor.

We would like to be able to predict the temperature distribution in the water (Tw) and the foam (Tf).

The heat transferred from the foam to the water will modeled as a heat loss and heat source term respectively.

i.e.

In the foam, the energy equation is

$$0 = \nabla \cdot \left(-k_f \nabla T_f \right) - \dot{q}_{loss}$$

and In the water, the energy equation is

$$0 = \nabla \cdot \left(-k_w \nabla T_w \right) - r C_p D T + \dot{q}_{gained}$$

The loss/source term is defined by a local heat transfer coefficient multiplied by the specific surface area (surface area per volume) multiplied by the difference between the water and the foam temperatures.

In other words, the source/loss term is defined as

$$\dot{q}_{loss} = \dot{q}_{gained} = -h_{loc} \cdot A_{spec} \cdot (T_f - T_w)$$

That defines the heat equations (2 unknowns and 2 equations). Now we must define the equations of continuity and momentum. The continuity equation for this problem is

$$\nabla \cdot v = 0$$

Lastly, the momentum equation through a porous media can be described by Brinkman, App. Sci. Research, A1, 27-34, 81-86 (1947) as a modification of Darcy's Law.

$$0 = -\nabla p - \frac{m}{k} v + m\nabla^2 v + r\mathbf{g}$$

This reduces to the standard momentum equation through an open channel as the permeability, κ, becomes sufficiently large as in a open channel.

i.e. $\kappa_f = 1e\text{-}8$

$\kappa_1 = \kappa_2 = 1e8$

Also, this momentum equation can be reduced to three equations, an x-component, a y-component and a z-component, leaving us now with 6 equations and 6 unknowns, i.e.

Unknowns are, v_x, v_y, v_z, P, T_f, T_w. (need 6 equations)

Equations:

(1), (2) (3) $0 = -\nabla p - \frac{m}{k} v + m\nabla^2 v + r\mathbf{g}$ (1 equation for each x,y,z vector)

(4) $\nabla \cdot v = 0$

(5) $0 = \nabla \cdot \left(-k_w \nabla T_w\right) - rC_p DT + \dot{q}_{gained}$

(6) $0 = \nabla \cdot \left(-k_f \nabla T_f\right) - \dot{q}_{loss}$

$$\dot{q}_{loss} = \dot{q}_{gained} = -h_{loc} \cdot A_{spec} \cdot (T_f - T_w)$$

This is a complicated model. Most researchers utilize a method where they do not model the foam exactly, but model the effect of the foam on the waters thermal conductivity. In other words, they simply model the effect of the foam on the pressure drop through the region and the flow of the fluid by the Brinkman equation, and then they assume that the water has a thermal conductivity in the foam region equivalent to the foam. This simplifies the model to the following.

(1), (2) (3) $$0 = -\nabla p - \frac{m}{k} v + m\nabla^2 v + r\mathbf{g}$$ (1 equation for each x,y,z velocity vector)

(4) $$\nabla \cdot v = 0$$

(5) $$0 = \nabla \cdot \left(-k_w \nabla T_w\right) - rC_p DT$$

8.2. Comparison:

The first model is a more complicated model, however, it takes into account the effect of the pore size, local heat transfer coefficient, and anisotropic thermal conductivity of the water. However, this model is very complex, and leads to very long times for the finite element programs to solve. The second model is a simpler model, easier to solve, but does not take into account the actual structure of the foam. Hence, the assumption of the second model is that the local heat transfer coefficient is sufficiently high that small changes in heat transfer (due to shedding, porosity effects on turbulence, etc.) are insignificant compared to the total surface area and thermal conductivity of the foam.

So, an experiment was run with both models under the same conditions. The results are presented in the following figures. Figure 1 is a plot of the average heater temperature [C] versus the Reynolds number of the flow. As can be seen, the two models correspond very closely, thus verifying the hypothesis that the internal heat transfer effects within the pores are insignificant compared to the global heat transfer due to the high conductivity of the foam. Hence, the simpler model may be substituted for the more complex model. One note to mention is that these models do not take into account any thermal resistance between the foam and the adhesive and the baseplate. The average heater temperature is actually the average temperature at the surface of the foam which is touching the baseplate. For more accurate predictions, these thermal resistance must be taken into account. Therefore, it would be useful to plot the thermal resistance of the foam with fluid flowing through it versus the flow parameters. This is shown in Figure 2. Figure 3 is a plot of the Stanton number versus Reynolds number, a common plot for heat transfer in porous media. Lastly, in heat transfer devices, the pumping power is extremely important, thus Figure 4 plots the thermal resistance versus pumping power. As can be seen, the

high pressure drop of the foam results in a very high pumping power. However, this now becomes an engineering problem. Figure 5 shows the transverse temperature profile in the foam region. As can be seen, a significant portion of the foam is relatively isothermal. Hence, if the foam height is reduced with the same velocity of water running through the remaining foam, the heat transfer should not change much. This is represented in Figure 6. This figure is striking, indicating that most of the heat is transferred to the fluid in the foam closest to the hot surface. From this plot is is indicated that the foam height really needs to be only 20% the foam length with the same velocity of fluid. Hence, this design would utilize only 20% of the fluid compared to the original design. Thus, pumping power is reduced with negligible effect on the heat transfer.

Last, the model was used to compare actual measured heat sinks to the predicted temperatures from the model. This is shown in Table I. As can be seen, the predictions are 4 different conditions are relatively accurate.

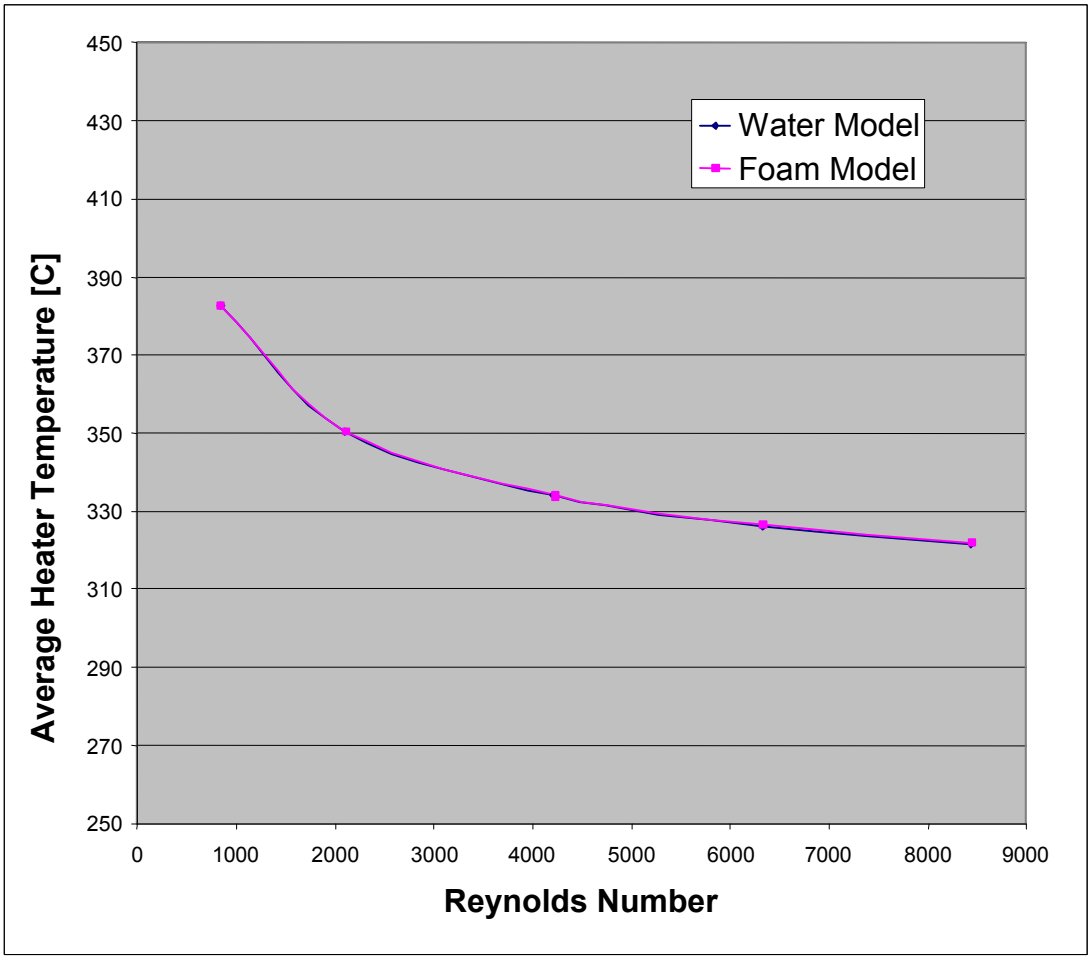

Figure A3. Average heater temperature versus Reynolds number.

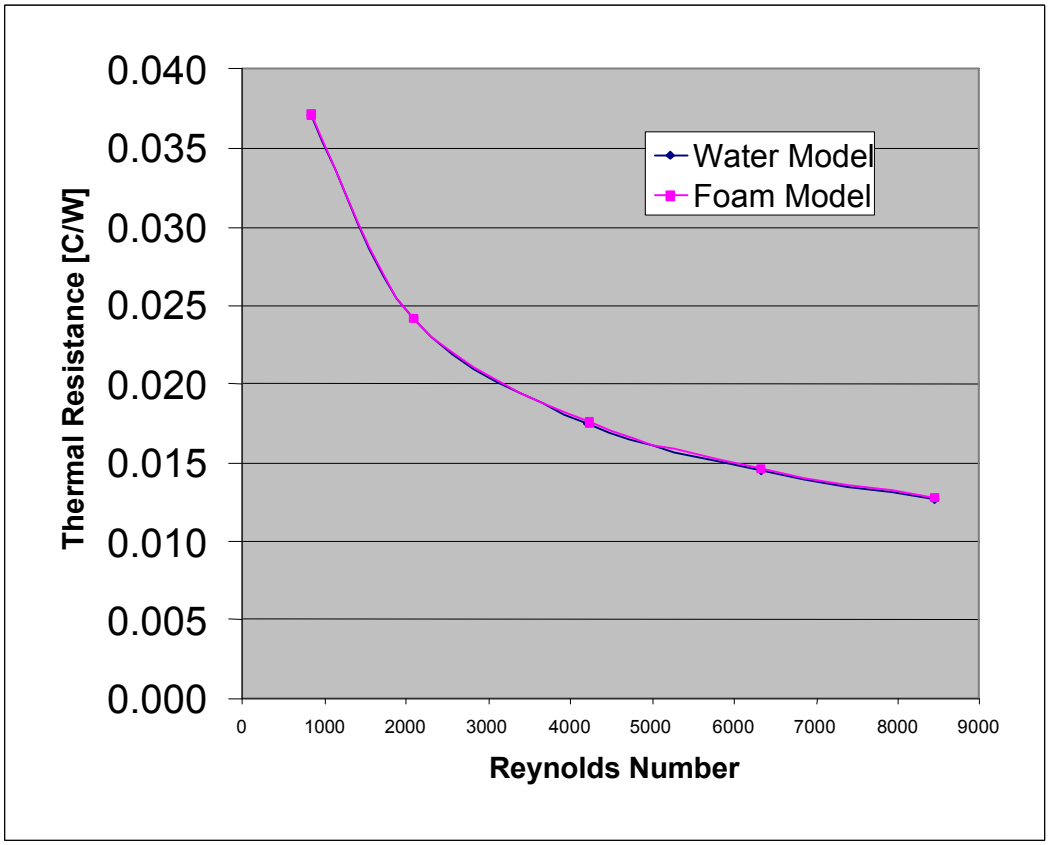

Figure A4. Thermal resistance of foam compared to Reynolds number for water flow.

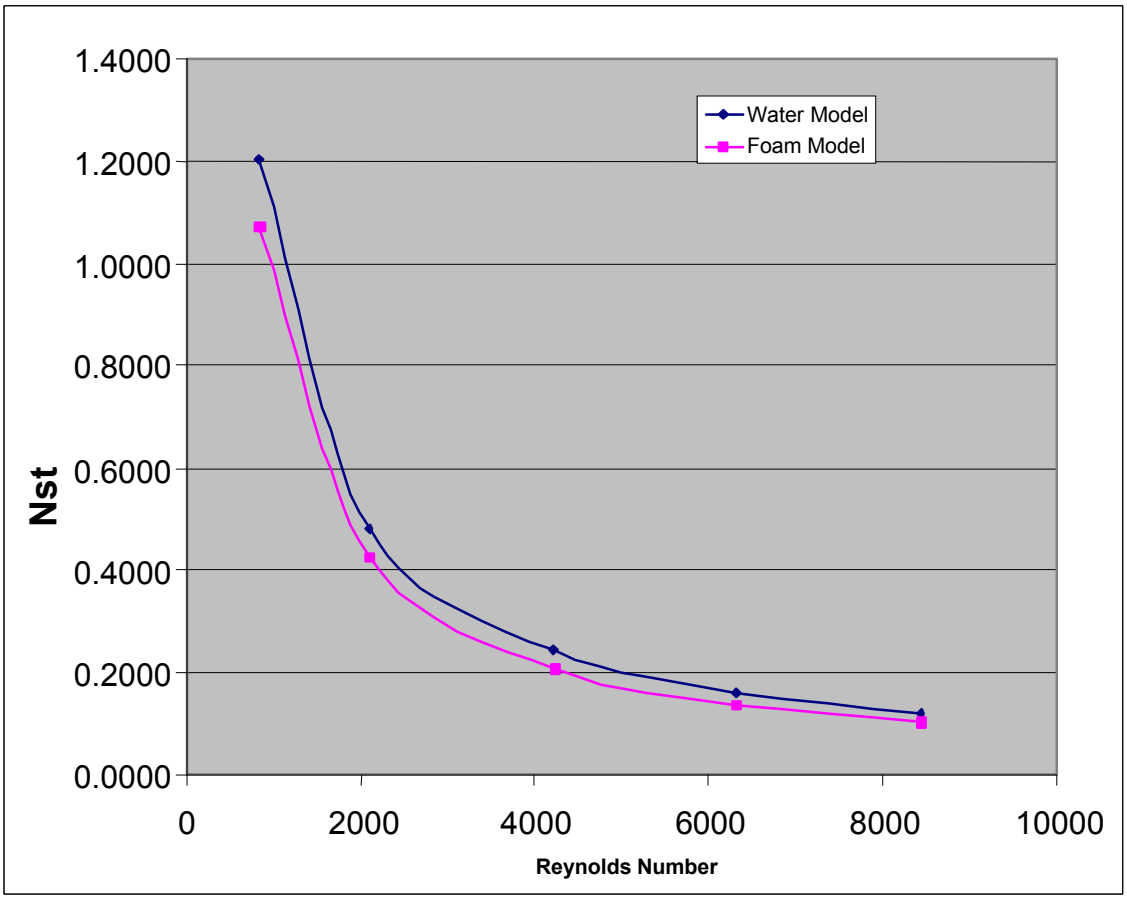

Figure A5. Stanton number versus Reynolds number of the foam with water flow.

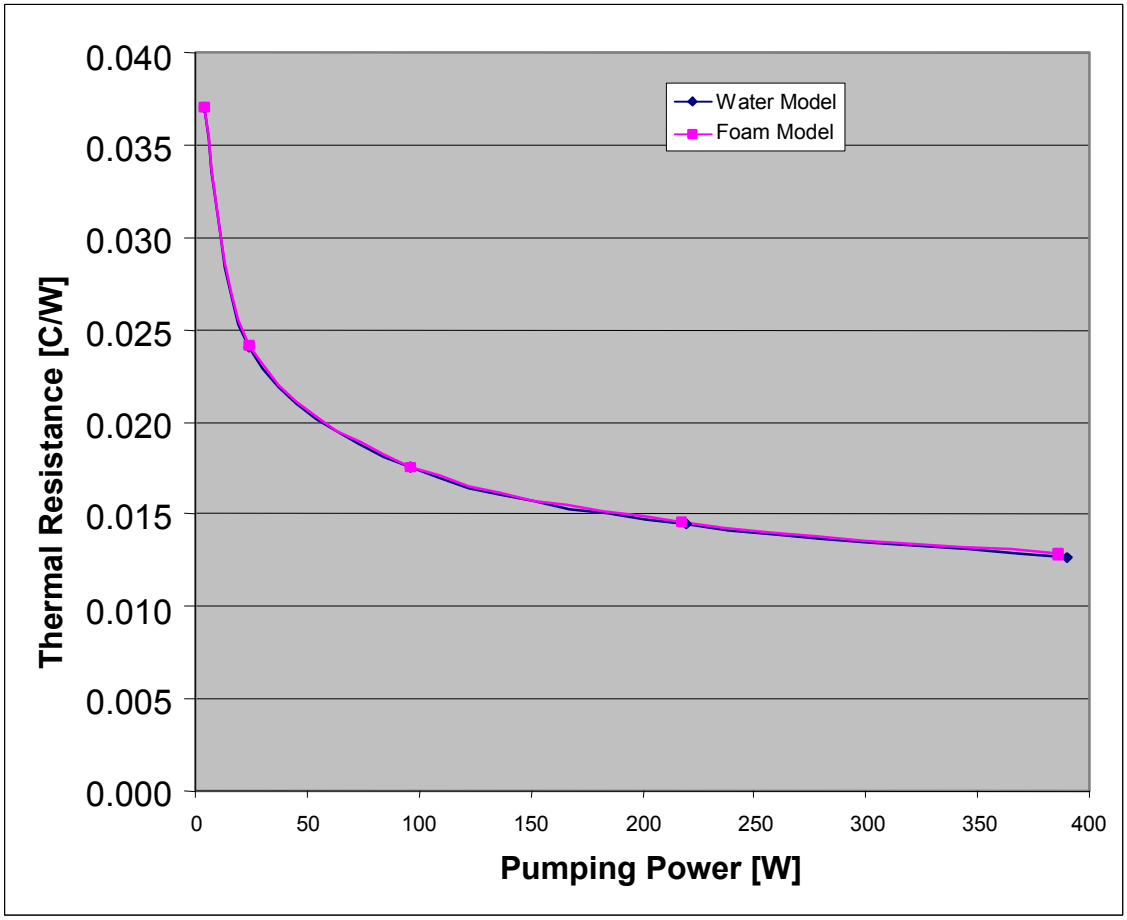

Figure A6. Thermal resistance versus pumping power.

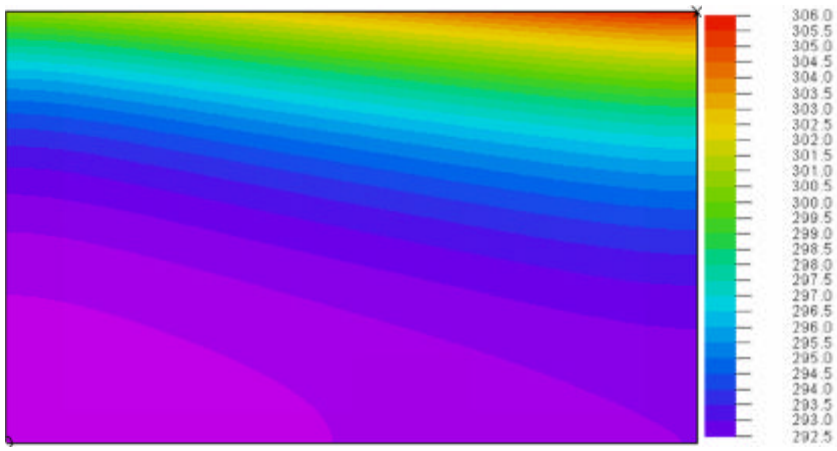

Figure A7. Plot of cross section temperature profile.

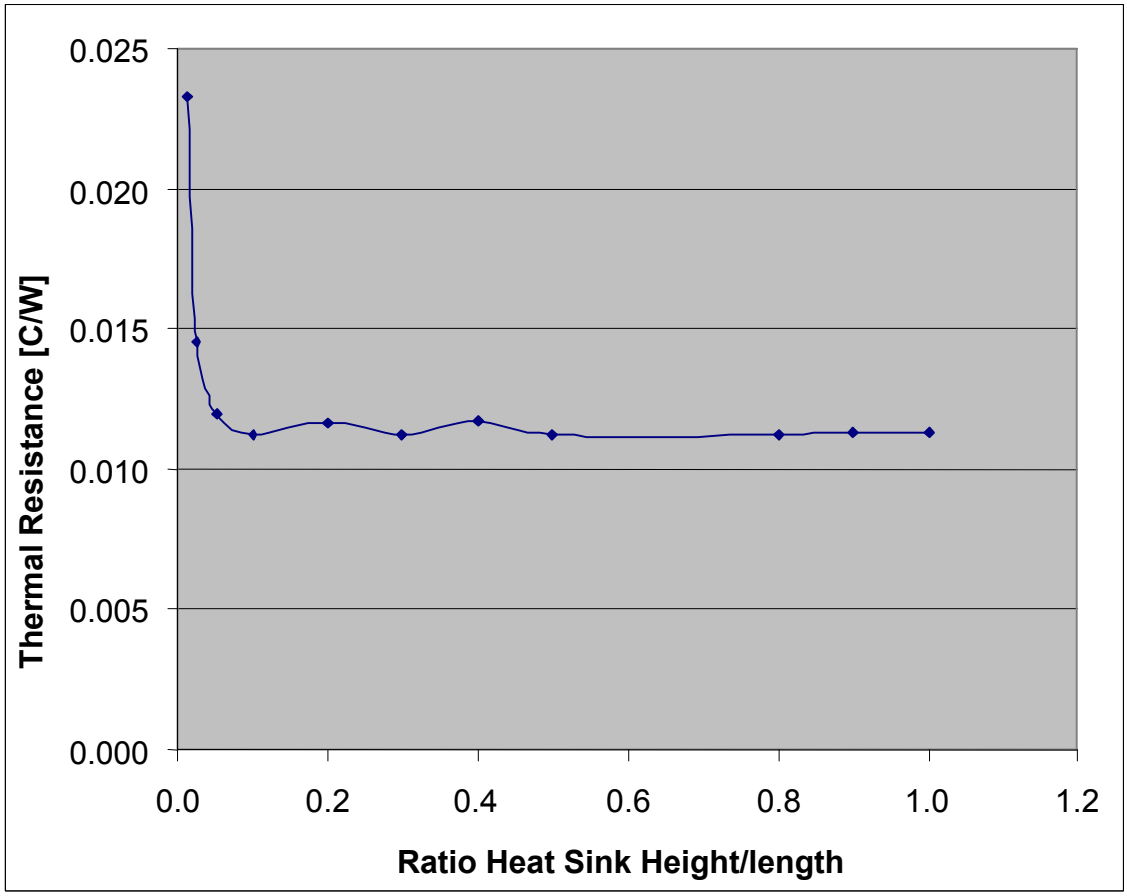

Figure A8. Plot of thermal resistance versus ratio of heat sink height/heat sink length.

Table I. Results of model compared to measured data.

Power Input	Water Flow Rate [gph]	Pressure Drop [psi]	Measured Base Plate Temperature [K]	Predicted Base Plate Temperature [K]	Measured Outlet Water Temperature [K]	Predicted Outlet Water Temperature [K]
300 W	**25**	**3.5**	**300.3**	**299.6**	**293.8**	**293.7**
300 W	**45**	**7.0**	**296.8**	**297.2**	**292.6**	**292.4**
600 W	**25**	**3.5**	**308.7**	**308.4**	**296.3**	**295.8**
600 W	**45**	**7.0**	**303.4**	**303.6**	**293.9**	**293.9**

DISTRIBUTION

INTERNAL

1. T.D. Burchell, Bldg. 4508, MS 6088.
2. P. A. Carpenter, Bldg. 4500N, MS 6269.
3. P. J. Hadley, Bldg. 4500S, MS 6161.
4. D. R. Johnson, Bldg. 4515, MS 6066.
5. J. W. Klett, Bldg. 4508, MS 6087.
6. T. M. Rosseel, 4500S, MS 6161.
7. P. S. Sklad, Bldg 4515, MS 6065.
8. D. P. Stinton, Bldg. 4515, MS 6063.
9. K. M. Wilson, 4500N, 6196.
10. Office Technical Information and Classification, Bldg 6011, MS 6283.

EXTERNAL

11. David Hamilton, DOE Office of Freedom Car and Vehicle Technologies, EE-2G, FORS.
12. Ron Smith, Materials Resources International, 811 W. Fifth Street, Unit 2, Lansdale, PA 19446.
13. DOE-WFO, G209